

Computational Models for Circadian Rhythms: Deterministic Versus Stochastic Approaches

Jean-Christophe Leloup, Didier Gonze,
and Albert Goldbeter

*Unité de Chronobiologie théorique, Faculté des
Sciences, Université Libre de Bruxelles, Brussels, Belgium*

Chapter 13

ABSTRACT

Circadian rhythms originate from intertwined feedback processes in genetic regulatory networks. Computational models of increasing complexity have been proposed for the molecular mechanism of these rhythms, which occur spontaneously with a period on the order of 24 h. We show that deterministic models for circadian rhythms in *Drosophila* account for a variety of dynamical properties, such as phase shifting or long-term suppression by light pulses and entrainment by light/dark cycles. Stochastic versions of these models allow us to examine how molecular noise affects the emergence and robustness of circadian oscillations. Finally, we present a deterministic model for the mammalian circadian clock and use it to address the dynamical bases of physiological disorders of the sleep/wake cycle in humans.

I. INTRODUCTION: THE COMPUTATIONAL BIOLOGY OF CIRCADIAN RHYTHMS

Most living organisms have developed the capability of generating autonomously sustained oscillations with a period close to 24 h. The function of these so-called *circadian rhythms* is to allow the organisms to adapt their physiology to the natural alternation of day and night. Circadian rhythms are endogenous because they can occur in constant environmental conditions (e.g., constant darkness). During the last two decades, experimental studies have shed much light on the molecular mechanism of circadian rhythms, which represents a long-standing problem in biology. In all eukaryotic organisms investigated so far, the molecular mechanism

of circadian oscillations relies on the negative feedback exerted by a clock protein on the expression of its gene (Hardin et al. 1990; Glossop et al. 1999; Lee et al. 2000; Alabadi et al. 2001; Reppert and Weaver 2002).

Even before details were known about their molecular origin, abstract mathematical models were used to probe the dynamic properties of circadian rhythms. A popular model of this type was provided by the van der Pol equations, which were originally proposed for sustained oscillations in electrical circuits. Thus, the van der Pol oscillator has been used for more than three decades for modeling circadian rhythms (e.g., to account for phase shifts of these rhythms by light pulses (Jewett and Kronauer 1998)). Another application involving this model pertains to modeling the enhanced fitness due to the resonance of circadian rhythms with the external light/dark cycle in cyanobacteria (Gonze et al. 2002c).

However, now that the molecular mechanism of circadian rhythms has largely been uncovered, mathematical models based on experimental observations have been proposed. Taking the form of a system of coupled ordinary differential equations, these deterministic models predict that in a certain range of parameter values the genetic regulatory network at the core of the clock mechanism can produce sustained oscillations of the limit cycle type. Deterministic models for circadian rhythms were first proposed for *Drosophila* and *Neurospora* (Goldbeter 1995, 1996; Leloup and Goldbeter 1998; Leloup et al. 1999; Smolen et al. 2001; Ueda et al. 2001), and later for mammals (Forger and Peskin 2003; Leloup and Goldbeter 2003, 2004; Becker-Weimann et al. 2004). The first model showing that oscillations can originate from negative feedback on gene expression was due to Goodwin (1965), who showed (already four decades ago) that periodic behavior may originate from such mode of genetic regulation. Modified versions of the Goodwin model are still being used to probe properties of circadian rhythms in organisms such as *Neurospora* (Ruoff et al. 2001). In this chapter we will focus on more recent models, which rely on more detailed molecular mechanisms.

One limitation of deterministic models is that they do not take into consideration the fact that the number of molecules involved in the regulatory mechanism within the rhythm-producing cells may be small as observed, for example, in *Neurospora* (Morrow et al. 1997). At low concentrations of protein or messenger RNA molecules, molecular fluctuations are likely to have a marked impact on circadian oscillations (Barkai and Leibler 2000). To assess the effect of molecular noise, it is necessary to resort to a stochastic approach. Comparing the predictions of deterministic and stochastic models for circadian rhythms shows that robust circadian oscillations can be observed even when the maximum number of mRNA and protein molecules is of the order of some tens and hundreds, respectively (Gonze et al. 2002a, 2002b, 2004a).

The goal of this chapter is to present an overview of deterministic and stochastic models for circadian rhythms. We will begin by presenting (in Section II) deterministic models for circadian oscillations of the PER protein and its mRNA in *Drosophila*. A core model will be presented, which also provides a useful model for circadian rhythms in *Neurospora*. This model for *Drosophila* circadian rhythms will

be extended to take into account the role of the TIM protein and the control of circadian behavior by light.

In Section III, we consider stochastic versions of these models. We examine how molecular noise affects the emergence of circadian oscillations and determine the influence of a variety of factors, such as number of protein and mRNA molecules, degree of cooperativity of repression, distance from bifurcation point, and rate constants characterizing the binding of the repressor protein to the gene. Two types of stochastic models are presented: one involves a fully detailed description of individual reaction steps, whereas a second relies on a non-developed description of nonlinear kinetic steps. Both types of models yield largely similar results. The study of stochastic models for circadian oscillations will allow us to characterize the domain of validity of deterministic models for circadian rhythms.

In Section IV we return to deterministic approaches and present a model for the mammalian circadian clock. We use this model to address the molecular bases of disorders of the sleep/wake cycle in humans, which are associated with dysfunctions of the clock. Computational models can thus be applied to investigating not only the molecular mechanism of circadian rhythms but the origin of associated physiological disorders. As discussed in Section V, the example of circadian rhythms illustrates how more and more complex models have been presented over the years to account for new experimental observations. We consider the need for such an increase in complexity of computational models for circadian rhythms, and the added insights these complex models provide for a better understanding of circadian behavior.

II. MODELING THE DROSOPHILA CIRCADIAN CLOCK

A. Overview of experimental observations

Some of the most remarkable advances in elucidating the molecular basis of circadian rhythms have been made in mutants of the fly *Drosophila* (Konopka 1979; Hall and Rosbash 1988; Baylies et al. 1993; Dunlap 1993), in which circadian rhythms affect the rest/activity cycle and the daily eclosion peaks of pupae. Both rhythms persist in constant darkness or temperature (Pittendrigh 1960). The classic work of Konopka and Benzer (1971) yielded *Drosophila* flies altered in their circadian system, owing to mutations in a single gene called *per* (for “period”). Four phenotypes were characterized: the wild type (per^+) has a free-running period of activity and eclosion close to 24 h; short-period mutants (per^s) have a period close to 19 h; in long-period mutants (per^l), the periodicity increases up to 29 h; and arrhythmic mutants (per^0) have lost the circadian pattern of eclosion or activity (Konopka and Benzer 1971; Konopka 1979). Interestingly, whereas in the wild type the period remains independent of temperature—a property known as temperature compensation, which is common to all circadian rhythms (Pittendrigh 1960)—the mutants per^l and per^s have lost this property (Konopka et al. 1989). In contrast to the wild

type, the period of their activity rhythm respectively increases and decreases with temperature. Accounting for temperature compensation of circadian rhythms remains an important challenge for computational biology.

A breakthrough for the mechanism of circadian rhythms in *Drosophila* was the finding (Hardin et al. 1990, 1992) that *per* mRNA is produced in a circadian manner. This periodic variation is accompanied by a circadian rhythm in the degree of abundance of PER. The peak in *per* mRNA precedes the peak in PER by 4 to 8 h (Zerr et al. 1990; Zeng et al. 1994). On the basis of this observation, Hardin et al. (1990, 1992) suggested that the *Drosophila* circadian rhythm results from a negative feedback exerted by the PER protein on the synthesis of the *per* mRNA. Post-translational modification of PER is also involved in the mechanism of circadian oscillations. Experimental evidence indeed indicates that PER is multiply phosphorylated (Edery et al. 1994). It appears that PER phosphorylation plays a role in the circadian oscillatory mechanism, by controlling the nuclear localization of PER and/or its degradation (Grima et al. 2002; Ko et al. 2002).

Overexpression of PER in *Drosophila* eyes represses *per* transcription and suppresses circadian rhythmicity in these cells, without affecting circadian oscillations in other *per*-expressing cells in the brain or the circadian rhythm in locomotor activity. This work shows that the action of PER on transcription is intracellular, and suggests that "each *per*-expressing cell contains an autonomous oscillator of which the *per* feedback loop is a component" (Zeng et al. 1994). Such a mechanism, based on negative autoregulation of transcription, has also been found in *Neurospora* (Aronson et al. 1994). The current view is that negative autoregulation of gene expression by a clock protein represents a unified mechanism for the generation of circadian rhythmicity in a wide variety of experimental systems (Dunlap 1999; Young and Kay 2001).

B. A core deterministic model for circadian oscillations of the PER protein and its mRNA

A first model for circadian oscillations in the *Drosophila* PER protein and its mRNA is based on multiple phosphorylation of PER and on the inhibition of *per* transcription by a phosphorylated form of the protein (Goldbeter 1995). This model, schematized in Figure 13.1a, can be viewed as a minimal core model because it takes into account a limited number of phosphorylated residues of PER. The model also applies to oscillations of FRQ and *frq* mRNA in *Neurospora*.

In the model, the *per* gene is first expressed in the nucleus and transcribed into *per* messenger RNA (mRNA). The latter is transported into the cytosol, where it is translated into the PER protein, P_0 , and degraded. The PER protein undergoes multiple phosphorylation, from P_0 into P_1 and from P_1 into P_2 . These modifications, catalyzed by a protein kinase, are reverted by a phosphatase. The fully phosphorylated form of the protein is marked up for degradation and transported into the nucleus in a reversible manner. The nuclear form of the protein (P_N) represses the transcription of the gene.

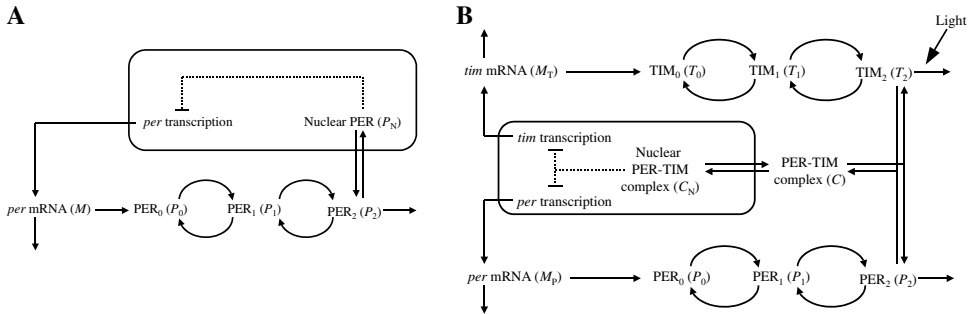


Figure 13.1. Schemes of the models for circadian oscillations in *Drosophila*. (a) The PER model is based on the sole negative regulation exerted by the PER protein on the expression of its gene (Goldbeter 1995). (b) The PER-TIM model incorporates the *tim* gene and its product, which forms a complex with the PER protein. This model is based on the negative regulation exerted by the PER-TIM complex on the expression of the *per* and *tim* genes. The effect of light is to increase the rate of TIM degradation (Leloup and Goldbeter 1998).

In the model, we consider two successive phosphorylations of PER, which is the minimal implementation of multiple phosphorylation. A single phosphorylation step would yield similar results. In fact, sustained oscillations can occur in the absence of phosphorylation, as shown by the study of a three-variable model representing an even simpler model for circadian oscillations (Leloup et al. 1999; Gonze and Goldbeter 2000; Gonze et al. 2000). We nevertheless focus on a model that includes multiple phosphorylation, because this process contributes to the mechanism of circadian oscillations by introducing a delay in the negative feedback loop.

In the model, the temporal variation of the concentrations of mRNA (M) and of the various forms of the regulatory protein—cytosolic (P_0 , P_1 , P_2) or nuclear (P_N)—is governed by the following system of kinetic equations (see Goldbeter (1995, 1996) for further details):

$$\begin{aligned}
 \frac{dM}{dt} &= v_s \frac{K_I^n}{K_I^n + P_N^n} - v_m \frac{M}{K_m + M} \\
 \frac{dP_0}{dt} &= k_s M - v_1 \frac{P_0}{K_1 + P_0} + v_2 \frac{P_1}{K_2 + P_1} \\
 \frac{dP_1}{dt} &= v_1 \frac{P_0}{K_1 + P_0} - v_2 \frac{P_1}{K_2 + P_1} - v_3 \frac{P_1}{K_3 + P_1} + v_4 \frac{P_2}{K_4 + P_2} \\
 \frac{dP_2}{dt} &= v_3 \frac{P_1}{K_3 + P_1} - v_4 \frac{P_2}{K_4 + P_2} - v_d \frac{P_2}{K_d + P_2} - k_1 P_2 + k_2 P_N \\
 \frac{dP_N}{dt} &= k_1 P_2 - k_2 P_N
 \end{aligned} \tag{13.1}$$

In these equations, the phosphorylation and dephosphorylation terms (with maximum rates v_1 , v_3 , and v_2 , v_4 , respectively)—as well as the degradation terms for

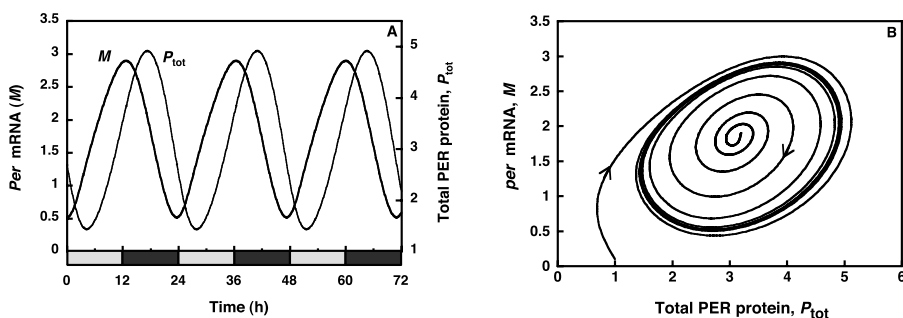


Figure 13.2. Sustained oscillations and limit cycle generated by the PER model. (a) Temporal variation in *per* mRNA (M) and in the total amount of PER protein (P_{tot}). (b) Sustained oscillations in total PER protein and *per* mRNA (expressed in nM) correspond to the evolution toward a limit cycle when the system's trajectory is projected onto the (M , P_{tot}) plane. Starting from two different initial conditions, the system reaches a unique closed curve characterized by a period and amplitude that are fixed for the given set of parameter values. The curves have been obtained by numerical integration of Equations 13.1. Parameter values are $v_s = 0.76$ nM/h, $v_m = 0.65$ nM/h, $k_s = 0.38$ h $^{-1}$, $v_d = 0.95$ nM/h, $k_1 = 1.9$ h $^{-1}$, $k_2 = 1.3$ h $^{-1}$, $K_1 = 1$ nM, $K_d = 0.2$ nM, $K_1 = K_2 = K_3 = K_4 = 2$ nM, $n = 4$, $V_1 = 3.2$ nM/h, $V_2 = 1.58$ nM/h, $V_3 = 5$ nM/h, and $V_4 = 2.5$ nM/h. Initial conditions are $M = 0.1$, $P_0 = P_1 = P_2 = P_N = 0.25$ ($P_{tot} = 1$), $M = 1.9$, and $P_0 = P_1 = P_2 = P_N = 0.8$ ($P_{tot} = 3.2$) (see Goldbeter (1995, 1996)).

mRNA and fully phosphorylated PER protein (with maximum rates v_m and v_d , respectively)—are all of Michaelian form corresponding to non-cooperative enzyme kinetics. The repression term takes the form of a Hill equation characterized by the Hill coefficient n . Repression by P_N becomes steeper and steeper as the degree of cooperativity n increases above unity. Although higher cooperativity favors the occurrence of sustained oscillations, periodic behavior can also be obtained for $n = 1$ (i.e., in the absence of cooperativity in repression).

For an appropriate set of parameter values, the model accounts for the occurrence of sustained oscillations in continuous darkness (Figure 13.2a). When plotting the time evolution of one variable (e.g., *per* mRNA (M)) as a function of another variable (e.g., the total amount of PER protein (P_{tot})), these oscillations correspond in such a phase plane to the evolution toward a closed curve, known as a limit cycle (Figure 13.2b). This name stems from the fact that the same closed trajectory is reached regardless of initial conditions, as illustrated in Figure 13.2b. In addition to accounting for the circadian rhythms in mRNA and for protein level, the model shows how variations in parameters such as the rate of degradation of PER or the rate of its translocation into the nucleus may change the period of the oscillations, or even suppress rhythmic behavior (Goldbeter 1995, 1996).

When the model based on PER alone was proposed, the way light affects circadian rhythms in *Drosophila* was still unknown. In 1996, a series of papers showed, concomitantly, that a second protein—TIM (for TIMELESS)—forms a complex with PER, and that light acts by inducing degradation of TIM (Hunter-Ensor et al. 1996; Lee et al. 1996; Myers et al. 1996; Zeng et al. 1996). These observations paved the

way for the construction of a more detailed computational model incorporating the formation of a PER-TIM complex as well as the enhancement of TIM degradation during the light phase.

C. A ten-variable deterministic model for circadian oscillations in *Drosophila*

The ten-variable model for circadian oscillations of the PER and TIM proteins and of *per* and *tim* mRNAs in *Drosophila* (Leloup and Goldbeter 1998; Leloup et al. 1999) is schematized in Figure 13.1b. The mechanism is based on the negative feedback exerted by the complex between the nuclear PER and TIM proteins on the expression of their genes. For each of these proteins, transcription, translation, and multiple phosphorylation are treated as in the PER model of Figure 13.1a. The fully phosphorylated proteins PER and TIM are marked up for degradation, and form a complex that is transported into the nucleus in a reversible manner. The nuclear form of the PER-TIM complex represses the transcription of the *per* and *tim* genes.

Recent experiments indicate that repression is in fact of indirect nature: a complex between two activators, the CLOCK and CYC proteins, promotes the expression of the *per* and *tim* genes. The PER-TIM complex prevents this activation by forming a complex with CLOCK and CYC (Darlington et al. 1998; Rutila et al. 1998; Lee et al. 1999). We return to the effect of such an indirect negative feedback in Section IV, restricting the present discussion to the PER-TIM model. In this model, the variables are the concentrations of the mRNAs (M_P and M_T), the various forms of the PER and TIM proteins ($P_0, P_1, P_2, T_0, T_1, T_2$), and the cytosolic (C) and nuclear (C_N) forms of the PER-TIM complex. The temporal evolution of the concentration variables is governed by the following system of 10 kinetic equations (see Leloup and Goldbeter (1998) and Leloup et al. (1999) for further details):

$$\begin{aligned}
 \frac{dM_P}{dt} &= v_{sP} \frac{K_{IP}^n}{K_{IP}^n + C_N^n} - v_{mP} \frac{M_P}{K_{mP} + M_P} - k_d M_P \\
 \frac{dP_0}{dt} &= k_{sP} M_P - V_{1P} \frac{P_0}{K_{1P} + P_0} + V_{2P} \frac{P_1}{K_{2P} + P_1} - k_d P_0 \\
 \frac{dP_1}{dt} &= V_{1P} \frac{P_0}{K_{1P} + P_0} - V_{2P} \frac{P_1}{K_{2P} + P_1} - V_{3P} \frac{P_1}{K_{3P} + P_1} + V_{4P} \frac{P_2}{K_{4P} + P_2} - k_d P_1 \\
 \frac{dP_2}{dt} &= V_{3P} \frac{P_1}{K_{3P} + P_1} - V_{4P} \frac{P_2}{K_{4P} + P_2} - k_3 P_2 T_2 + k_4 C - v_{dP} \frac{P_2}{K_{dP} + P_2} - k_d P_2 \\
 \frac{dM_T}{dt} &= v_{sT} \frac{K_{IT}^n}{K_{IT}^n + C_N^n} - v_{mT} \frac{M_T}{K_{mT} + M_T} - k_d M_T \\
 \frac{dT_0}{dt} &= k_{sT} M_T - V_{1T} \frac{T_0}{K_{1T} + T_0} + V_{2T} \frac{T_1}{K_{2T} + T_1} - k_d T_0 \\
 \frac{dT_1}{dt} &= V_{1T} \frac{T_0}{K_{1T} + T_0} - V_{2T} \frac{T_1}{K_{2T} + T_1} - V_{3T} \frac{T_1}{K_{3T} + T_1} + V_{4T} \frac{T_2}{K_{4T} + T_2} - k_d T_1
 \end{aligned} \tag{13.2}$$

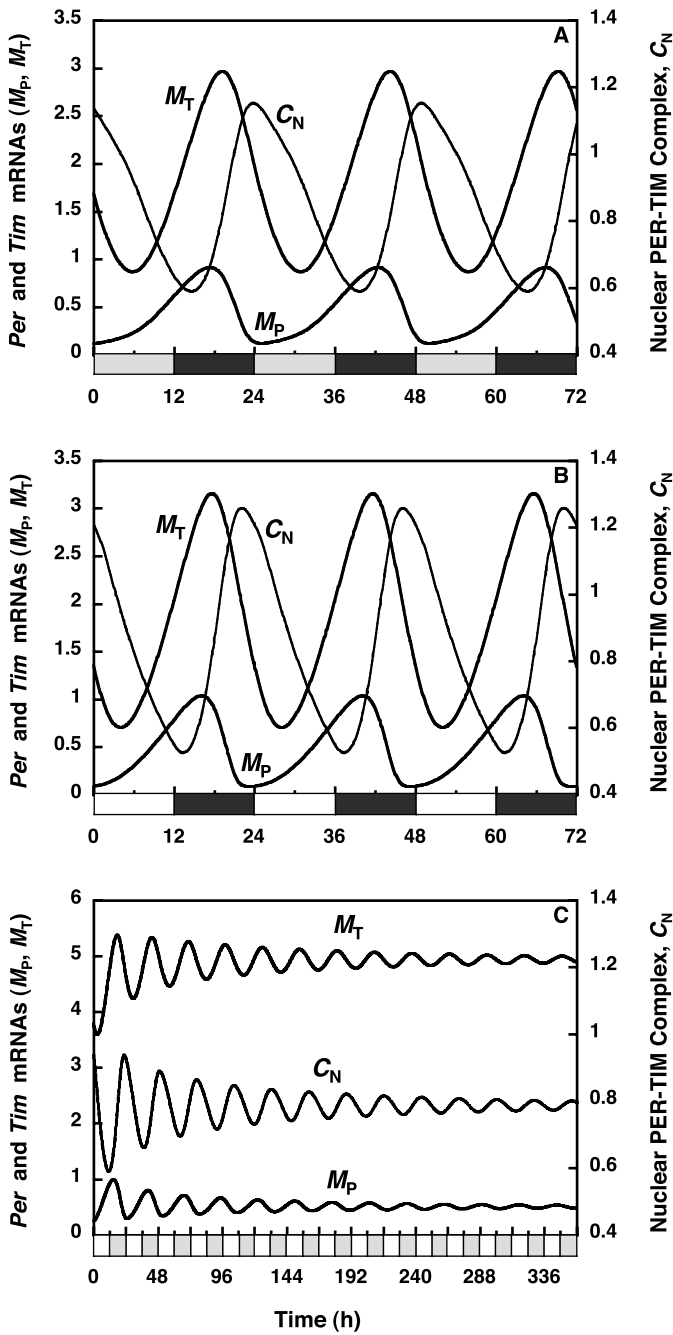
$$\begin{aligned}\frac{dT_2}{dt} &= V_{3T} \frac{T_1}{K_{3T} + T_1} - V_{4T} \frac{T_2}{K_{4T} + T_2} - k_3 P_2 T_2 + k_4 C - v_{dT} \frac{T_2}{K_{dT} + T_2} - k_d T_2 \\ \frac{dC}{dt} &= k_3 P_2 T_2 - k_4 C - k_1 C + k_2 C_N - k_{dC} C \\ \frac{dC_N}{dt} &= k_1 C - k_2 C_N - k_{dN} C_N\end{aligned}$$

These equations correspond to one particular version in a family of possible models, which differ by details of the molecular implementation of the feedback mechanism. Thus, rather than considering the formation of a complex between the fully phosphorylated forms of PER and TIM the complex could be made also (or instead) between the non-phosphorylated or mono-phosphorylated forms of the proteins. These other versions of the basal model yield largely similar results.

The various terms appearing in Equations 13.2 are similar to those of Equations 13.1. We have added nonspecific degradation terms, characterized by the rate constants k_d , k_{dC} , and k_{dN} . These linear terms are generally of negligible magnitude, and are not essential for oscillations. Their inclusion ensures the existence of a steady state when the specific protein degradation processes are inhibited. In Equations 13.2, parameter v_{dT} represents the maximum value of the TIM degradation rate. This is the light-sensitive parameter, which will be set to a constant low value during continuous darkness, and to a constant high value during continuous light. In a light/dark cycle, v_{dT} will vary in a square-wave manner between these two extreme values. The square-wave corresponds well to laboratory conditions under which light varies in an all-or-none manner. The natural variation of light is of course smoother, and other waveforms should be considered to address the effect of variations of luminosity under natural light/dark cycles.

Much as the PER model, the model based on the formation of the PER-TIM complex can account for sustained autonomous oscillations originating from negative auto-regulatory feedback. Now, however, we may address the dynamic behavior of the model in various lighting conditions, by incorporating suitable changes in parameter v_{dT} . Thus, as illustrated in Figure 13.3, sustained oscillations can occur

Figure 13.3. Circadian oscillations in the PER-TIM model. From top to bottom, the curves correspond to (a) sustained oscillations in continuous darkness, (b) entrainment by a light/dark cycle of 24 h period (12 : 12 LD), and (c) damped oscillations in continuous light. The LD cycle is symbolized by the alternation of white and black bars. Continuous darkness is symbolized by the alternation of gray and black bars. Shown is the temporal variation in *per* and *tim* mRNAs (M_P , M_T) and in the concentration of nuclear PER-TIM complex (C_N). The curves have been obtained by numerical integration of Equations 13.2 (Leloup and Goldbeter 1998). Parameter values are $v_{SP} = 0.8 \text{ nM h}^{-1}$, $v_{ST} = 1 \text{ nM h}^{-1}$, $v_{MP} = 0.8 \text{ nM h}^{-1}$, $v_{MT} = 0.7 \text{ nM h}^{-1}$, $K_{MP} = K_{MT} = 0.2 \text{ nM}$, $k_{SP} = k_{ST} = 0.9 \text{ h}^{-1}$, $v_{dP} = v_{dT} = 2 \text{ nM h}^{-1}$, $k_1 = 1.2 \text{ h}^{-1}$, $k_2 = 0.2 \text{ h}^{-1}$, $k_3 = 1.2 \text{ nM}^{-1} \text{ h}^{-1}$, $k_4 = 0.6 \text{ h}^{-1}$, $K_{IP} = K_{IT} = 1 \text{ nM}$, $K_{dP} = K_{dT} = 0.2 \text{ nM}$, $n = 4$, $K_{1P} = K_{1T} = K_{2P} = K_{2T} = K_{3P} = K_{3T} = K_{4P} = K_{4T} = 2 \text{ nM}$, $k_d = k_{dC} = k_{dN} = 0.01 \text{ h}^{-1}$, $V_{1P} = V_{1T} = 8 \text{ nM h}^{-1}$, $V_{2P} = V_{2T} = 1 \text{ nM h}^{-1}$, $V_{3P} = V_{3T} = 8 \text{ nM h}^{-1}$, and $V_{4P} = V_{4T} = 1 \text{ nM h}^{-1}$. Parameter v_{dT} is increased from 2 nM/h in the dark phase to 5 nM/h in the light phase (Leloup and Goldbeter 1998).



in continuous darkness (DD), but damped oscillations occur in conditions corresponding to continuous light (LL), as observed in *Drosophila* (Qiu and Hardin 1996). In LL, the light-sensitive parameter was chosen so that it takes a high value corresponding to a stable steady state. The disappearance of oscillations can be explained intuitively: because of enhanced degradation, the TIM protein cannot reach a level allowing effective repression by the PER-TIM complex. Oscillations observed in DD with a period close to 24 h can be entrained by a 12 : 12 LD cycle (12 h of light followed by 12 h of darkness). Experimentally, there exists a window of entrainment, ranging typically from 21 to 28 h (Moore-Ede et al. 1982).

The PER-TIM model allows us to compare theoretical predictions with experimental observations in a variety of cases. A first comparison pertains to entrainment by LD cycles of varying photoperiod. As shown by the experiments of Qiu and Hardin (1996), the peak in *per* mRNA always follows the transition from the L to the D phase by about 4 h. A similar result is obtained in the PER-TIM model (Figure 13.4). The lag after the L to D transition appears to be the same regardless of the duration of the light phase, because the level of TIM has decreased to a minimum value at the end of the L phase, and the time required for the PER-TIM complex to accumulate during the dark phase above the threshold for repression remains unchanged.

Another key comparison pertains to the phase shifts induced by light pulses in continuous darkness. Depending on the phase at which these perturbations are made, circadian oscillations can be either advanced or delayed. Alternatively, no phase shift may occur. These data yield a phase response curve (PRC) when the phase shift is plotted as a function of the phase of perturbation. The PRC is an

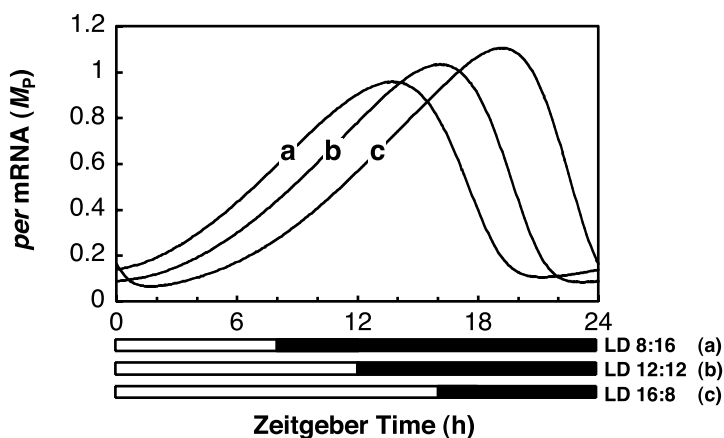


Figure 13.4. Phase locking of the *per* mRNA oscillations in the PER-TIM model. The three curves correspond to entrainment by a light/dark cycle of 24 h period but with different photoperiod: (a) 8 : 16 LD cycle, (b) 12 : 12 LD cycle, and (c) 16 : 8 LD cycle. The LD cycles are symbolized by the alternation of white and black bars. The curves have been obtained by numerical integration of Equations 13.2. Parameter values are as in Figure 13.3.

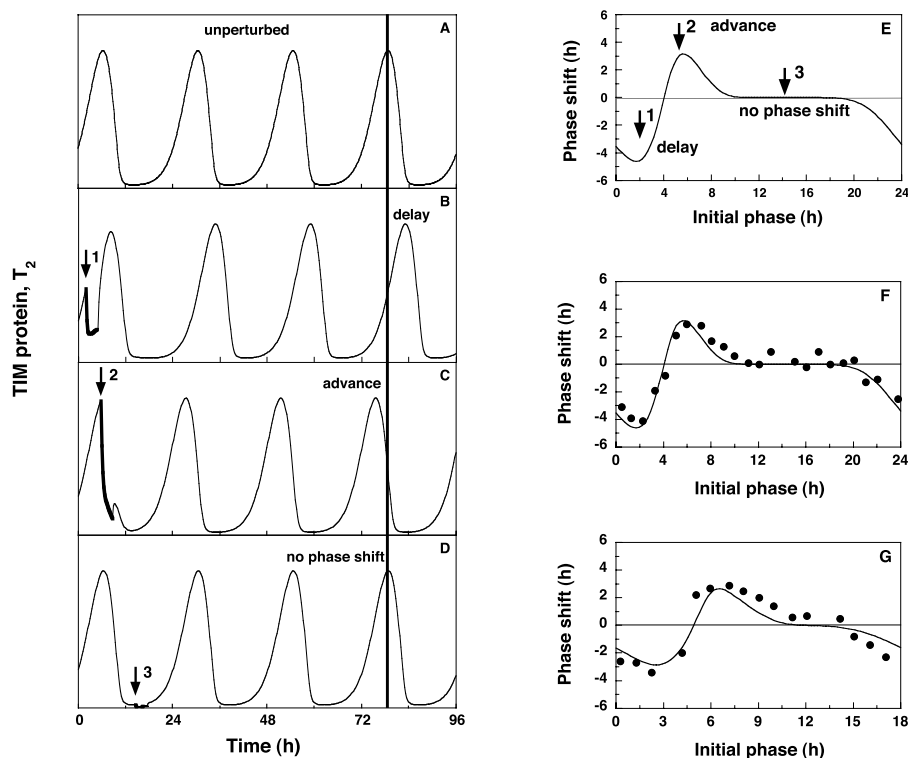


Figure 13.5. Phase shifting by a light pulse comparison with experiments. (a) Unperturbed oscillations of phosphorylated TIM (T_2). The vertical line through the fourth peak serves as reference for determining phases shifts. (b–d) Transient perturbations at three different phases of the oscillations, producing, respectively, a phase delay, a phase advance, or an absence of phase shift. The arrows mark the beginning of the light pulse and the thick lines indicate both the duration and the effect of this perturbation (see following). (e) Phase response curve (PRC) obtained by plotting the phase shift as a function of the phase at which the perturbation is applied. The perturbation takes the form of a 3-h twofold increase in TIM maximum degradation rate (v_{dT}), triggered by the light pulse. (f and g) PRCs obtained theoretically (solid lines) for the wild type (panel F) and for the *per^s* mutant (panel G) in *Drosophila*. The theoretical predictions compare well with the experimental observations (dots) based on data obtained by Konopka and Orr using a 1-min light pulse (redrawn from Figure 2 of Hall and Rosbash (1987)). The oscillations of the TIM protein (panels A– through D) and the PRCs (panels E through G) have been obtained by numerical integration of Equations 13.2 (Leloup and Goldbeter 1998). Parameter values are listed in Figure 2 of Leloup and Goldbeter (1998). For the PRCs, the zero phase is chosen, as in the experiments (Hall and Rosbash 1987), so that the minimum in *per* mRNA occurs after 12 h.

important tool in the study of circadian rhythms. We may simulate the effect of light pulses in the PER-TIM model by transiently increasing the maximum rate of TIM degradation, v_{dT} . Unperturbed oscillations of fully phosphorylated TIM (T_2) are shown in Figure 13.5a, where the vertical line through the fourth peak will serve as reference for determining phase shifts triggered by transient perturbations.

As shown in Figure 13.5b, when the perturbation is applied during the rising phase of TIM a phase delay is observed. In contrast, a phase advance occurs when the perturbation is made at the maximum of TIM (Figure 13.5c), whereas no phase shift is observed when the pulse is given at the minimum of TIM (Figure 13.5d). The latter result stems from the fact that when TIM is already at its minimum a transient increase in TIM degradation remains without effect. Plotting the phase shifts as a function of the phase of perturbation yields the PRC shown in Figure 13.5e, where the arrows 1 through 3 refer to the situations depicted in panels B through D, respectively. The predictions of the model compare well with the experimental PRC both for wild-type flies (Figure 13.5f, where the solid curve is the same PRC as in panel E) and for the *per^s* mutant (Figure 13.5g). The model indicates that the dead zone in which no phase shift occurs is nearly absent in the *per^s* mutant because TIM remains near its minimum for a relatively much shorter time, as a result of the faster degradation of PER in this mutant (see Figure in Leloup and Goldbeter (1998)).

Obtaining good agreement with experimental observations is not straightforward, as this requires an appropriate characterization of the biochemical effects of a light pulse on the circadian clock. In constructing the theoretical PRC of Figure 13.5, we assumed that the effect of the light pulse is to double during 3 h the maximum rate of TIM degradation. Other combinations of multiplication factor and duration of increase may also yield satisfactory agreement. The interest of this result is to predict that the light pulse should have long-lasting biochemical consequences that may outlast the light pulse itself. This prediction is in fact corroborated by recent experimental observations (Busza et al. 2004).

Other results obtained with the PER-TIM model are of a more counter-intuitive nature. First, the model shows that in a certain range of parameter values sustained oscillations of the limit cycle type may coexist with a stable steady state. Such a situation, known as hard excitation, provides a possible explanation for the suppression of circadian rhythms by a single light pulse and for the subsequent restoration of periodic behavior by a second such pulse. This puzzling phenomenon, which has been observed in a variety of organisms, remains largely unexplained. The model indicates that over a range of phases corresponding to TIM increase in *Drosophila* transient increases in parameter v_{dT} may bring the system from the limit cycle into the basin of attraction of the stable steady state. A second pulse in v_{dT} may then bring back the oscillations (Figure 13.6a). Suppression is only possible over a finite portion of the limit cycle, as shown in Figure 13.6b. The characteristics (duration and amplitude) of the suppressing pulse change with the phase of perturbation in this domain (Leloup and Goldbeter 2001). In contrast, a single critical perturbation suppressing the rhythm exists in the situation described by Winfree (1980), wherein the stable limit cycle surrounds an unstable steady state. However, suppression is only transient in that case. The coexistence between a stable steady state and a stable limit cycle (illustrated in Figure 13.6a) is by no means uncommon, but a computational model is clearly needed to predict the occurrence of such a phenomenon.

We were at first surprised to observe that the deterministic PER-TIM model was also capable of producing chaotic behavior in constant environmental conditions

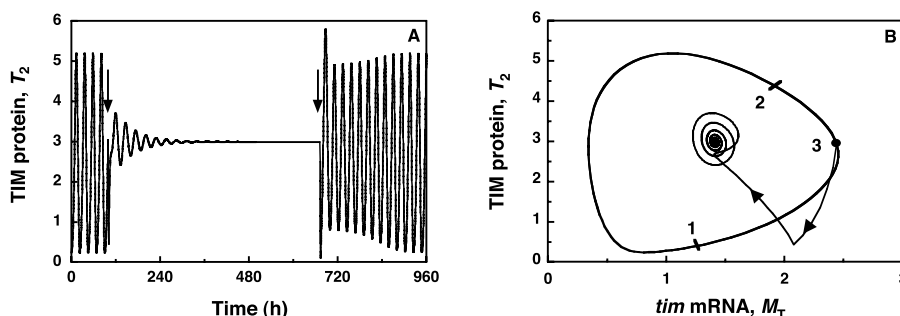


Figure 13.6. Long-term suppression of circadian rhythms by a single pulse of light. (a) Permanent rhythm suppression by a single pulse of light in the PER-TIM model, and restoration of the rhythm by a similar pulse. At the time indicated by the first arrow, to mimic the effect of a light pulse parameter v_{dT} , which measures the maximum rate of TIM degradation, is increased during 2 h from the basal value of 1.3 nM h^{-1} up to 4.0 nM h^{-1} . Initial conditions correspond to point 3 in panel B. At the time indicated by a second arrow, a similar change in v_{dT} , mimicking a second light pulse, is initiated, and the system returns to the oscillatory regime. The curve is obtained by numerical integration of Equations 13.2 for the parameter values of Figure 4 in Leloup and Goldbeter (2001). (b) Light pulses, translated into transient increases in v_{dT} , can permanently suppress the rhythm when applied over a portion of the limit cycle bounded by the two black bars marked 1 and 2. The trajectory starting from point 3 on the limit cycle corresponds to the rhythm suppression by the first pulse in a.

(e.g., continuous darkness (Leloup and Goldbeter 1999)). Such autonomous chaos has previously been shown to originate from the interplay between two instability-generating mechanisms (e.g., two feedback loops, each of which may produce sustained oscillations (Goldbeter 1996)). Here, the model contains but a single negative feedback loop, exerted by the PER-TIM complex. However, the formation of this complex involves two branches leading to the synthesis of PER and TIM. Chaos occurs in a relatively small parameter domain when a dynamical imbalance arises between the synthesis and degradation of the PER and TIM proteins or their mRNAs. Nonautonomous chaos can also be found in models for circadian rhythms, as a result of the periodic forcing of the circadian clock by light/dark cycles. The theoretical study indicates (Gonze and Goldbeter 2000) that the occurrence of such nonautonomous chaos is favored by the square wave nature of LD cycles: the domain of entrainment indeed enlarges at the expense of the domain of chaos when the waveform of the LD cycle progressively changes from square wave to sinusoidal.

Another use of the PER and PER-TIM models for circadian oscillations in *Drosophila* is to address the dynamical bases of temperature compensation (i.e., the relative independence of the period of circadian oscillations with respect to temperature (see Section II.A)). The analysis of the models supports the view (Ruoff and Rensing 1996) that temperature compensation originates from a balance between two opposing tendencies: the acceleration of some reactions with temperature tends to increase the period, whereas the acceleration of other reactions tends to lower it (Leloup and Goldbeter 1997). When the balance is lost (as a

result of a mutation), temperature compensation fails to occur, as observed in long- and short-period *Drosophila* mutants.

This discussion shows how useful deterministic models of moderate complexity may prove for the study of circadian rhythms. However, the question arises as to the validity of these computational models when the numbers of molecules involved in the oscillatory mechanism are small, as may occur for proteins and mRNAs in cellular conditions. Then, deterministic models may reach their limits, and it becomes necessary to resort to stochastic approaches. We shall now examine how stochastic models may account for the emergence of circadian rhythms, and will turn thereafter to more complex deterministic models proposed for the mammalian circadian clock.

III. STOCHASTIC MODELS FOR CIRCADIAN RHYTHMS

A. Core molecular model for circadian oscillations

To illustrate the stochastic approach to modeling circadian rhythms, it will be useful to resort to a relatively simple model for circadian oscillations. The model examined in Section II.A and schematized in Figure 13.1a provides a core model for circadian rhythms based on the negative feedback exerted by a protein (which is referred to in the following as clock protein) on the expression of its gene. As previously indicated, this model applies to circadian oscillations of the PER protein and *per* mRNA in *Drosophila*, and to the case of *Neurospora* (Leloup et al. 1999, Gonze et al. 2000) for which circadian rhythms originate from the negative feedback exerted by the FRQ protein on the expression of its gene (Aronson et al. 1994; Lee et al. 2000). The core model contains five variables and is described by Equations 13.1. When the effect of light is incorporated—as was done for the PER-TIM model discussed in Section II.B—this model accounts for the occurrence of sustained oscillations in continuous darkness, phase-shifting by light pulses, and entrainment by light/dark cycles. The model shown in Figure 13.1a will thus serve as a convenient core model for testing the effect of molecular noise on circadian oscillations. An even simpler model (governed by a set of three kinetic equations) is obtained when disregarding multiple phosphorylation of the clock protein (Leloup et al. 1999; Gonze et al. 2000). The following discussion pertains to the five-variable model, which includes PER reversible phosphorylation.

B. Molecular noise in the fully developed stochastic version of the core model

The decrease in the total number (N) of molecules in a system of chemical reactions is accompanied by a rise in the amplitude of fluctuations around the state predicted by the deterministic evolution of this chemical system. These fluctuations, which reflect intrinsic molecular noise, can be taken into account by describing the chemical reaction system as a birth-and-death stochastic process governed by a

master equation (Nicolis and Prigogine 1977). In a given reaction step, molecules of participating species are either produced (birth) or consumed (death). At each step is associated a transition probability proportional to the numbers of molecules of involved chemical species and to the chemical rate constant of the corresponding deterministic model.

To implement such a master equation approach to stochastic chemical dynamics, Gillespie (1976, 1977) introduced a rigorous numerical algorithm. In addition to other approaches (Morton-Firth and Bray 1998), this method of the Monte Carlo type is widely used to determine the effect of molecular noise on the dynamics of chemical (Baras et al. 1990; Baras 1997), biochemical (McAdams and Arkin 1997), or genetic (Arkin et al. 1998) systems. The Gillespie method associates a probability with each reaction. At each time step the algorithm stochastically determines the reaction that takes place according to its probability, as well as the time interval to the next reaction. The numbers of molecules of the different reacting species as well as the probabilities are updated at each time step. In this approach (Gillespie 1976, 1977), a parameter denoted Ω permits the modulation of the number of molecules present in the system.

To assess the effect of molecular noise on circadian oscillations, we have used the Gillespie method to perform stochastic simulations of the core deterministic model governed by Equations 13.1. When the degree of cooperativity of repression—given by the Hill coefficient n in Equations 13.1—is equal to 4, the core mechanism can be decomposed in 30 elementary steps, as indicated in Table 13.1. A probability of occurrence, proportional to the deterministic rate constant, is associated with each of these individual steps. This approach rests on the analysis of a fully developed stochastic version of the core model for circadian oscillations. In the following we will show that an alternative (more compact) approach—in which the nonlinear functions in Equations 13.1 are not decomposed into elementary steps—yields largely similar results.

C. Robustness of circadian oscillations with respect to molecular noise

The first result obtained with the fully developed stochastic version of the core model for circadian rhythms is that it is also capable of producing sustained oscillations in conditions of continuous darkness. These oscillations correspond to the evolution toward a limit cycle, which is shown in the right-hand panels of Figure 13.7b as a projection onto the (M, P_N) plane. For comparison, the deterministic oscillations and the corresponding limit cycle are shown in Figure 13.7a. The effect of molecular noise is merely to induce variability in the maxima of the oscillations. This is reflected by the noisy appearance of the limit cycle and a thickening of its upper portion linking the maximum in mRNA with the maximum in nuclear (or total) clock protein. The noisy stochastic limit cycle surrounds the deterministic limit cycle (shown as the closed white curve in the lower right-hand panel in Figure 13.7b) obtained by numerical integration of Equations 13.1 in corresponding conditions (Gonze et al. 2002a, 2002b).

Table 13.1. Decomposition of the deterministic model into elementary reaction steps.

Reaction Number	Reaction Step	Probability of Reaction
1	$G + P_N \xrightarrow{a_1} GP_N$	$w_1 = a_1 \times G \times P_N / \Omega$
2	$GP_N \xrightarrow{d_1} G + P_N$	$w_2 = d_1 \times GP_N$
3	$GP_N + P_N \xrightarrow{a_2} GP_{N2}$	$w_3 = a_2 \times GP_N \times P_N / \Omega$
4	$GP_{N2} \xrightarrow{d_2} GP_N + P_N$	$w_4 = d_2 \times GP_{N2}$
5	$GP_{N2} + P_N \xrightarrow{a_3} GP_{N3}$	$w_5 = a_3 \times GP_{N2} \times P_N / \Omega$
6	$GP_{N3} \xrightarrow{d_3} GP_{N2} + P_N$	$w_6 = d_3 \times GP_{N3}$
7	$GP_{N3} + P_N \xrightarrow{a_4} GP_{N4}$	$w_7 = a_4 \times GP_{N3} \times P_N / \Omega$
8	$GP_{N4} \xrightarrow{d_4} GP_{N3} + P_N$	$w_8 = d_4 \times GP_{N4}$
9	$[G, GP_N, GP_{N2}, GP_{N3}] \xrightarrow{v_s} M$	$w_9 = v_s \times (G + GP_N + GP_{N2} + GP_{N3})$
10	$M + E_m \xrightarrow{k_{m1}} C_m$	$w_{10} = k_{m1} \times M \times E_m / \Omega$
11	$C_m \xrightarrow{k_{m2}} M + E_m$	$w_{11} = k_{m2} \times C_m$
12	$C_m \xrightarrow{k_{m3}} E_m$	$w_{12} = k_{m3} \times C_m$
13	$M \xrightarrow{k_5} M + P_0$	$w_{13} = k_5 \times M$
14	$P_0 + E_1 \xrightarrow{k_{11}} C_1$	$w_{14} = k_{11} \times P_0 \times E_1 / \Omega$
15	$C_1 \xrightarrow{k_{12}} P_0 + E_1$	$w_{15} = k_{12} \times C_1$
16	$C_1 \xrightarrow{k_{13}} P_1 + E_1$	$w_{16} = k_{13} \times C_1$
17	$P_1 + E_2 \xrightarrow{k_{21}} C_2$	$w_{17} = k_{21} \times P_1 \times E_2 / \Omega$
18	$C_2 \xrightarrow{k_{22}} P_1 + E_2$	$w_{18} = k_{22} \times C_2$
19	$C_2 \xrightarrow{k_{23}} P_0 + E_2$	$w_{19} = k_{23} \times C_2$
20	$P_1 + E_3 \xrightarrow{k_{31}} C_3$	$w_{20} = k_{31} \times P_1 \times E_3 / \Omega$
21	$C_3 \xrightarrow{k_{32}} P_1 + E_3$	$w_{21} = k_{32} \times C_3$
22	$C_3 \xrightarrow{k_{33}} P_2 + E_3$	$w_{22} = k_{33} \times C_3$
23	$P_2 + E_4 \xrightarrow{k_{41}} C_4$	$w_{23} = k_{41} \times P_2 \times E_4 / \Omega$
24	$C_4 \xrightarrow{k_{42}} P_2 + E_4$	$w_{24} = k_{42} \times C_4$
25	$C_4 \xrightarrow{k_{43}} P_1 + E_4$	$w_{25} = k_{43} \times C_4$
26	$P_2 + E_d \xrightarrow{k_{d1}} C_d$	$w_{26} = k_{d1} \times P_2 \times E_d / \Omega$
27	$C_d \xrightarrow{k_{d2}} P_2 + E_d$	$w_{27} = k_{d2} \times C_d$
28	$C_d \xrightarrow{k_{d3}} E_d$	$w_{28} = k_{d3} \times C_d$
29	$P_2 \xrightarrow{k_1} P_N$	$w_{29} = k_1 \times P_2$
30	$P_N \xrightarrow{k_2} P_2$	$w_{30} = k_2 \times P_N$

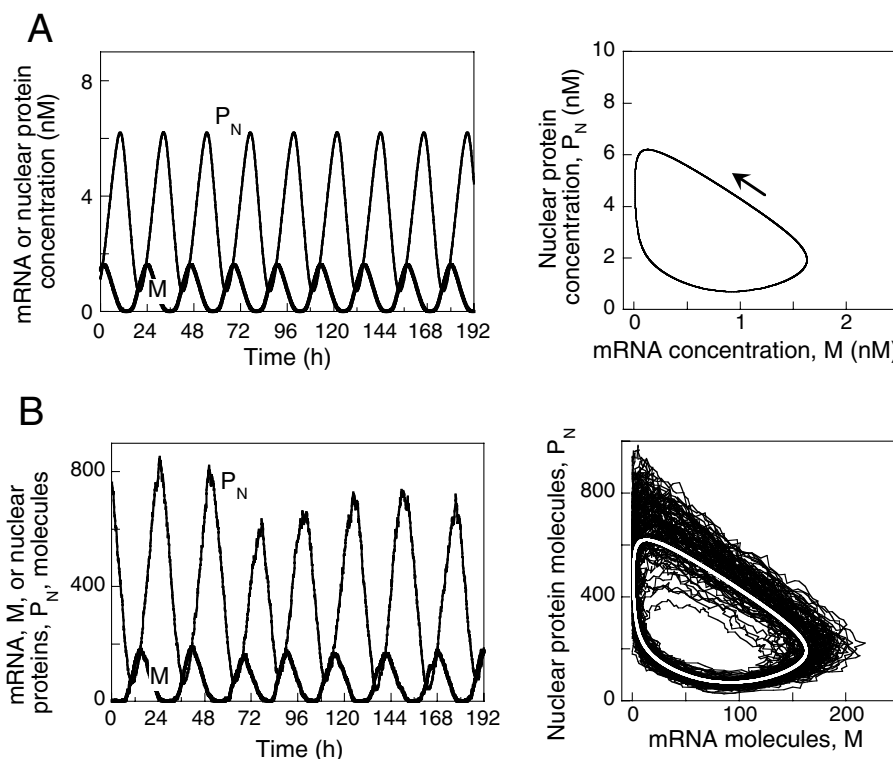


Figure 13.7. Deterministic versus stochastic simulations of the core model for circadian oscillations (schematized in Figure 13.1a). (a) Oscillations obtained in the absence of noise for the deterministic model governed by Equations 13.1. Sustained oscillations of mRNA (M) and nuclear clock protein (P_N) in the left-hand panel correspond to the evolution toward a limit cycle shown as a projection onto the (M, P_N) plane in the right-hand panel. (b) Oscillations generated by the stochastic version of the core model in the presence of noise, for $\Omega = 100$ and $n = 4$. The data, expressed in numbers of molecules of mRNA and of nuclear clock protein, are obtained by stochastic simulations of the detailed reaction system (Table 13.1) corresponding to the deterministic version of the core model. In the lower right-hand panel, the white curve corresponds to the deterministic limit cycle. The latter is surrounded by the stochastic trajectory which takes the form of a noisy limit cycle.

To assess the robustness of circadian oscillations at low numbers of molecules, we performed stochastic simulations for decreasing values of Ω . For $\Omega = 500$, the number of mRNA molecules varies in the range 0- to 1,000, whereas the numbers of nuclear and total clock protein molecules oscillate in the ranges 200 to 4,000 and 800- to 8,000, respectively (see left-hand panel in Figure 13.8a). The results in Figure 13.8 show that as Ω decreases progressively from the value of 500 down to a value of 100 or 50 robust circadian oscillations continue to occur in continuous darkness. The number of mRNA molecules oscillates from 0 to 200 or 0 to 120, whereas the number of nuclear clock protein molecules oscillates in the range 20 to 800 or 10

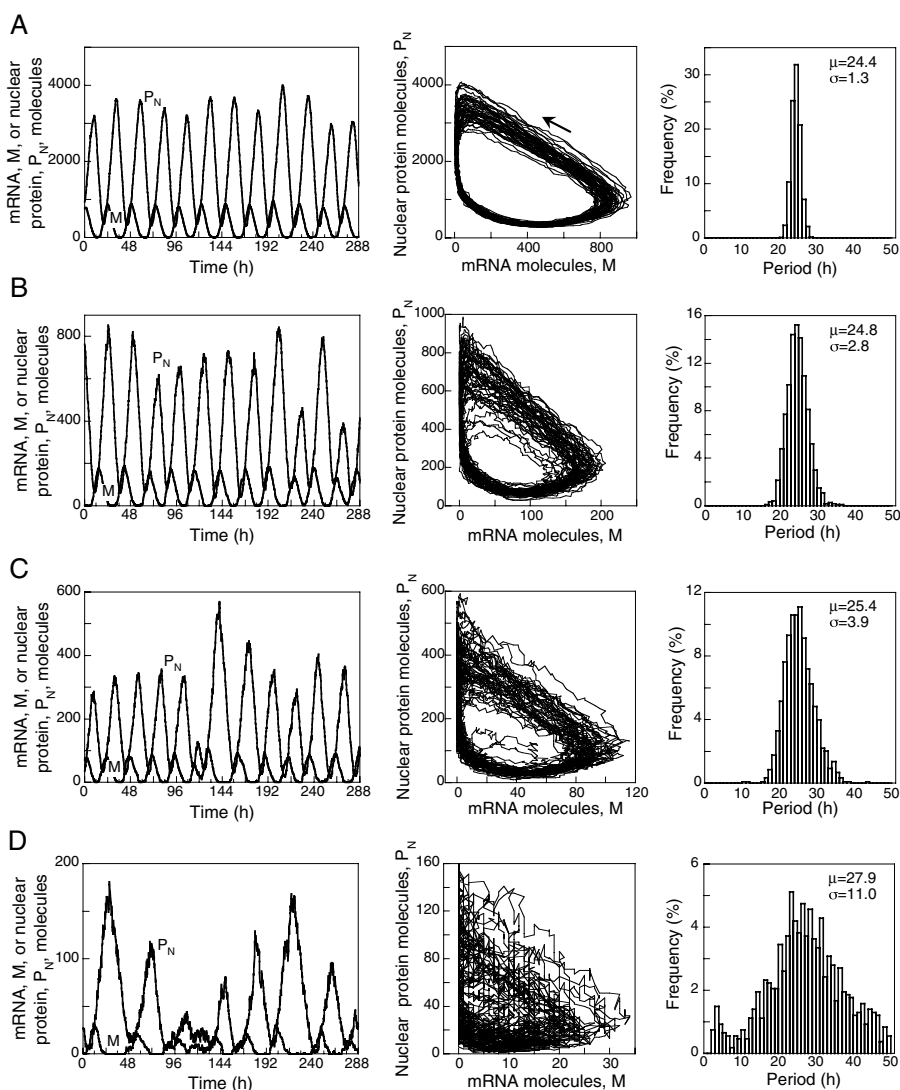


Figure 13.8. Effect of number of molecules on the robustness of circadian oscillations. Shown in rows A through D are the oscillations in the numbers of molecules of mRNA and nuclear clock protein, the projection of the corresponding limit cycle, and the histogram of periods of 1,200 successive cycles, for Ω varying from 500 (A), to 100 (B), 50 (C), and 10 (D). The curves are obtained by stochastic simulations of the core model (Table 13.1), for $n = 4$ (other parameters are listed in Table 13.2 where “mol” stands for “molecule”). For period histograms, the period was determined as the time interval separating two successive upward crossings of the mean level of mRNA or clock protein. In B and C, the decrease in the numbers of mRNA and protein molecules still permits robust circadian oscillations (see histograms where the mean value (μ) and standard deviation (σ) of the period are indicated in h), whereas at still lower numbers of molecules (D) noise begins to obliterate rhythmic behavior (Gonze et al. 2002b).

Table 13.2. Parameter values for stochastic simulations.

Reaction Steps	Parameter Values
Steps 1–8	<p>For $n = 4$:</p> $a_1 = \Omega \text{ mol}^{-1} \text{ h}^{-1}, d_1 = (160 \times \Omega) \text{ h}^{-1},$ $a_2 = (10 \times \Omega) \text{ mol}^{-1} \text{ h}^{-1}, d_2 = (100 \times \Omega) \text{ h}^{-1},$ $a_3 = (100 \times \Omega) \text{ mol}^{-1} \text{ h}^{-1}, d_3 = (10 \times \Omega) \text{ h}^{-1},$ $a_4 = (100 \times \Omega) \text{ mol}^{-1} \text{ h}^{-1}, d_4 = (10 \times \Omega) \text{ h}^{-1}$ <p>For $n = 3$:</p> $a_1 = \Omega \text{ mol}^{-1} \text{ h}^{-1}, d_1 = (80 \times \Omega) \text{ h}^{-1},$ $a_2 = (100 \times \Omega) \text{ mol}^{-1} \text{ h}^{-1}, d_2 = (100 \times \Omega) \text{ h}^{-1},$ $a_3 = (100 \times \Omega) \text{ mol}^{-1} \text{ h}^{-1}, d_3 = \Omega \text{ h}^{-1}$ <p>For $n = 2$:</p> $a_1 = \Omega \text{ mol}^{-1} \text{ h}^{-1}, d_1 = (40 \times \Omega) \text{ h}^{-1},$ $a_2 = (100 \times \Omega) \text{ mol}^{-1} \text{ h}^{-1}, d_2 = (10 \times \Omega) \text{ h}^{-1}$ <p>For $n = 1$:</p> $a_1 = (10 \times \Omega) \text{ mol}^{-1} \text{ h}^{-1}, d_1 = (20 \times \Omega) \text{ h}^{-1}$
Step 9	$v_s = (0.5 \times \Omega) \text{ mol h}^{-1}$
Steps 10–12	$k_{m1} = 165 \text{ mol}^{-1} \text{ h}^{-1}, k_{m2} = 30 \text{ h}^{-1}, k_{m3} = 3 \text{ h}^{-1},$ $E_{m \text{ tot}} = E_m + C_m = (0.1 \times \Omega) \text{ mol}$
Steps 13	$k_s = 2.0 \text{ h}^{-1}$
Steps 14–16	$k_{11} = 146.6 \text{ mol}^{-1} \text{ h}^{-1}, k_{12} = 200 \text{ h}^{-1}, k_{13} = 20 \text{ h}^{-1}$ $E_{1 \text{ tot}} = E_1 + C_1 = (0.3 \times \Omega) \text{ mol}$
Steps 17–19	$k_{21} = 82.5 \text{ mol}^{-1} \text{ h}^{-1}, k_{22} = 150 \text{ h}^{-1}, k_{23} = 15 \text{ h}^{-1},$ $E_{2 \text{ tot}} = E_2 + C_2 = (0.2 \times \Omega) \text{ mol}$
Steps 20–22	$k_{31} = 146.6 \text{ mol}^{-1} \text{ h}^{-1}, k_{32} = 200 \text{ h}^{-1}, k_{33} = 20 \text{ h}^{-1},$ $E_{3 \text{ tot}} = E_3 + C_3 = (0.3 \times \Omega) \text{ mol}$
Steps 23–25	$k_{41} = 82.5 \text{ mol}^{-1} \text{ h}^{-1}, k_{42} = 150 \text{ h}^{-1}, k_{43} = 15 \text{ h}^{-1},$ $E_{4 \text{ tot}} = E_4 + C_4 = (0.2 \times \Omega) \text{ mol}$
Steps 26–28	$k_{d1} = 1650 \text{ mol}^{-1} \text{ h}^{-1}, k_{d2} = 150 \text{ h}^{-1}, k_{d3} = 15 \text{ h}^{-1},$ $E_{d \text{ tot}} = E_d + C_d = (0.1 \times \Omega) \text{ mol}$
Steps 29–30	$k_1 = 2.0 \text{ h}^{-1}, k_2 = 1.0 \text{ h}^{-1}$

to 600. For these smaller values of Ω , the limit cycles are more noisy but the period histograms calculated for some 1,200 successive cycles indicate that the distribution remains narrow with a mean free running period μ close to a circadian value. The standard deviation σ remains small with respect to the mean period but slightly increases as the number of molecules diminishes.

A further decrease in the number of molecules (e.g., down to $\Omega = 10$) will eventually obliterate circadian rhythmicity, and the latter is overcome by noise (Figure 13.8d). At such a low value of Ω , highly irregular oscillations occur, during which the number of mRNA molecules varies from 0 to 30 and the number of nuclear protein

molecules oscillates in the range 5 to 160. Even for such reduced numbers of mRNA and protein molecules, however, oscillations are not fully destroyed by noise. The histogram of periods indicates that the mean is still close to a circadian value, but the standard deviation is greatly increased. The stochastic approach illustrated in Figures 13.7 and 13.8 provides us with the unique opportunity of witnessing the emergence of a biological rhythm out of molecular noise (Gonze et al. 2004a, 2004b).

The results in Figure 13.8 were obtained in conditions in which the mean levels of mRNA and of clock protein differ by one to two orders of magnitude. Similar results are obtained by means of stochastic simulations when the level of mRNA is considerably lower than that of the clock protein, as long as the former remains above a few tens of molecules.

The degree of cooperativity is another parameter that affects the robustness of circadian oscillations in the presence of molecular noise. Stochastic simulations were performed with $\Omega = 100$ for values of n ranging from 1 to 4, where n denotes the total number of protein molecules that bind to the promoter to repress transcription. The results indicate that robustness significantly increases when n passes from 1 (absence of cooperativity) to values of 2 and above. Changes in standard deviation of the period show that cooperative repression enhances the robustness of circadian oscillations with respect to molecular noise (Gonze et al. 2002b).

Stochastic simulations further indicate that circadian oscillations can be entrained by LD cycles. The effect of light is incorporated into the model by assuming that the probability of occurrence of the reaction step corresponding to degradation of phosphorylated clock protein increases during the light phase, as observed in *Drosophila*. Of particular interest is that the phase of the entrained rhythm is then stabilized through periodic forcing by the LD cycle (Figure 13.9). The phase of the maximum in mRNA of clock protein is of course not constant in these conditions, because of fluctuations, but its mean value occurs a few hours after the L-to-D transition, as observed in the case of *Drosophila* (see also Figure 13.4 for the results obtained in the corresponding deterministic case).

Additional factors influence the robustness of circadian oscillations with respect to molecular noise. Among these are the distance from a bifurcation point, and the magnitude of the rate constants characterizing binding of the repressor to the gene. To illustrate the first aspect, it is useful to consider the bifurcation diagram showing the onset of sustained oscillations as a function of a control parameter such as the maximum rate of clock protein degradation, v_d (Figure 13.10). This diagram, obtained for the core deterministic model of Figure 13.1a governed by Equations 13.1, shows that as v_d is progressively increased from a low initial value the system at first settles in a stable non-oscillatory state before sustained oscillations of the limit cycle type arise when v_d exceeds a critical value. The amplitude of the oscillations progressively increases as the value of v_d moves away from this bifurcation point. We now select four increasing values of v_d located well below (a) or just below (b) the bifurcation value, and just above (c) or well beyond (d) it. Stochastic simulations performed for a given value of Ω with the fully developed

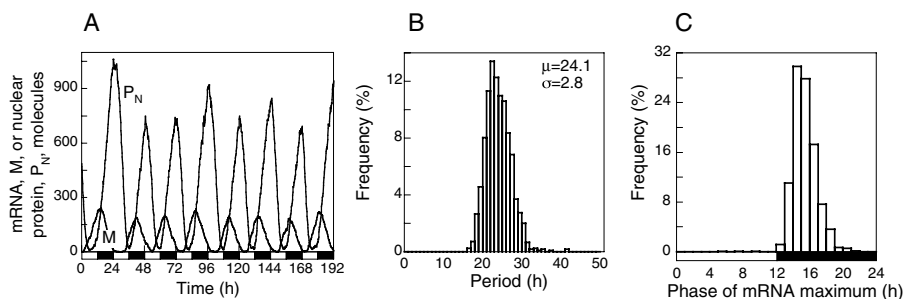


Figure 13.9. Effect of molecular noise on circadian oscillations under conditions of periodic forcing by a light/dark cycle. The data are obtained for $\Omega = 100$ and $n = 4$. (a) Circadian oscillations in the numbers of mRNA and nuclear clock protein molecules. (b) Histogram of periods with mean value (μ) and standard deviation (σ) indicated in h. (c) Histogram of the time corresponding to the maximum number of mRNA molecules over a period. Periodic forcing is achieved by doubling during each light phase the value ascribed during the dark phase to the parameter (k_{ds}) measuring the probability of the protein degradation step (Table 13.1). Histograms are determined for some 1,200 successive cycles (Gonze et al. 2002b).

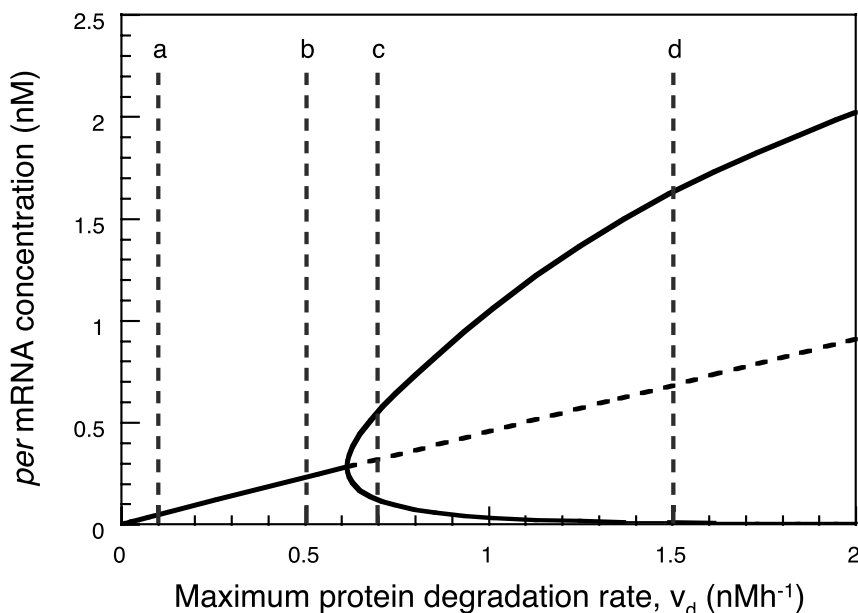


Figure 13.10. Bifurcation diagram showing the onset of sustained oscillations in the deterministic core model for circadian rhythms, as a function of parameter v_d (which measures the maximum rate of protein degradation). The curve shows the steady-state level of *per* mRNA, stable (solid line), or unstable (dashed line), as well as the maximum and minimum concentration of *per* mRNA in the course of sustained circadian oscillations. The diagram is established by means of the program AUTO (Doedel 1981) applied to Equations 13.1. Parameter values are given in Table 13.2 (Gonze et al. 2002a).

version of the core model indicate (Figure 13.11) that circadian oscillations become less sensitive to molecular noise as the system moves away from the bifurcation point, well into the domain of periodic behavior.

Finally, among the kinetic parameters that govern the probability of occurrence of the various individual steps listed in Table 13.1 few have as much influence on the robustness of circadian oscillations as the rate constants characterizing the successive binding of repressor molecules to the gene promoter of the clock protein. In the case of cooperative binding of four repressor molecules, we have to consider four successive steps of association and dissociation characterized by the rate constants a_i and d_i ($i = 1, \dots, 4$) (see steps 1 through 8 in Table 13.1). It will be useful to divide these rate constants by a scaling parameter γ to assess their influence on the robustness of circadian rhythms with respect to molecular noise. An increase in γ will thus correspond to a decrease in the rate constants a_i and d_i .

In Figure 13.12 are shown the results of stochastic simulations of the core model for $\gamma = 1$ (a), $\gamma = 100$ (b), and $\gamma = 1000$ (c). As γ increases up to 100 and 1,000, oscillations with larger and larger amplitude and increasing variability of the period are observed. The oscillations obtained for $\gamma = 1$ are much more regular. To clarify the nature of this phenomenon, we examined the deterministic version of the detailed stochastic model considered in Table 13.1. To the 30 reaction steps listed in Table 13.1 corresponds a deterministic system of 22 ordinary differential equations (Gonze et al. 2004a). In this fully developed version of the deterministic model, parameters a_i and d_i appear explicitly, whereas they only appear in the form of a single equilibrium inhibition constant (K) in the reduced five-variable deterministic model governed by Equations 13.1.

The results obtained with the fully developed deterministic model demonstrate the existence of a bifurcation as a function of the scaling parameter γ , as shown by the bifurcation diagram in Figure 13.13. When γ increases above a critical value close to 100, the system ceases to oscillate and evolves toward a stable steady


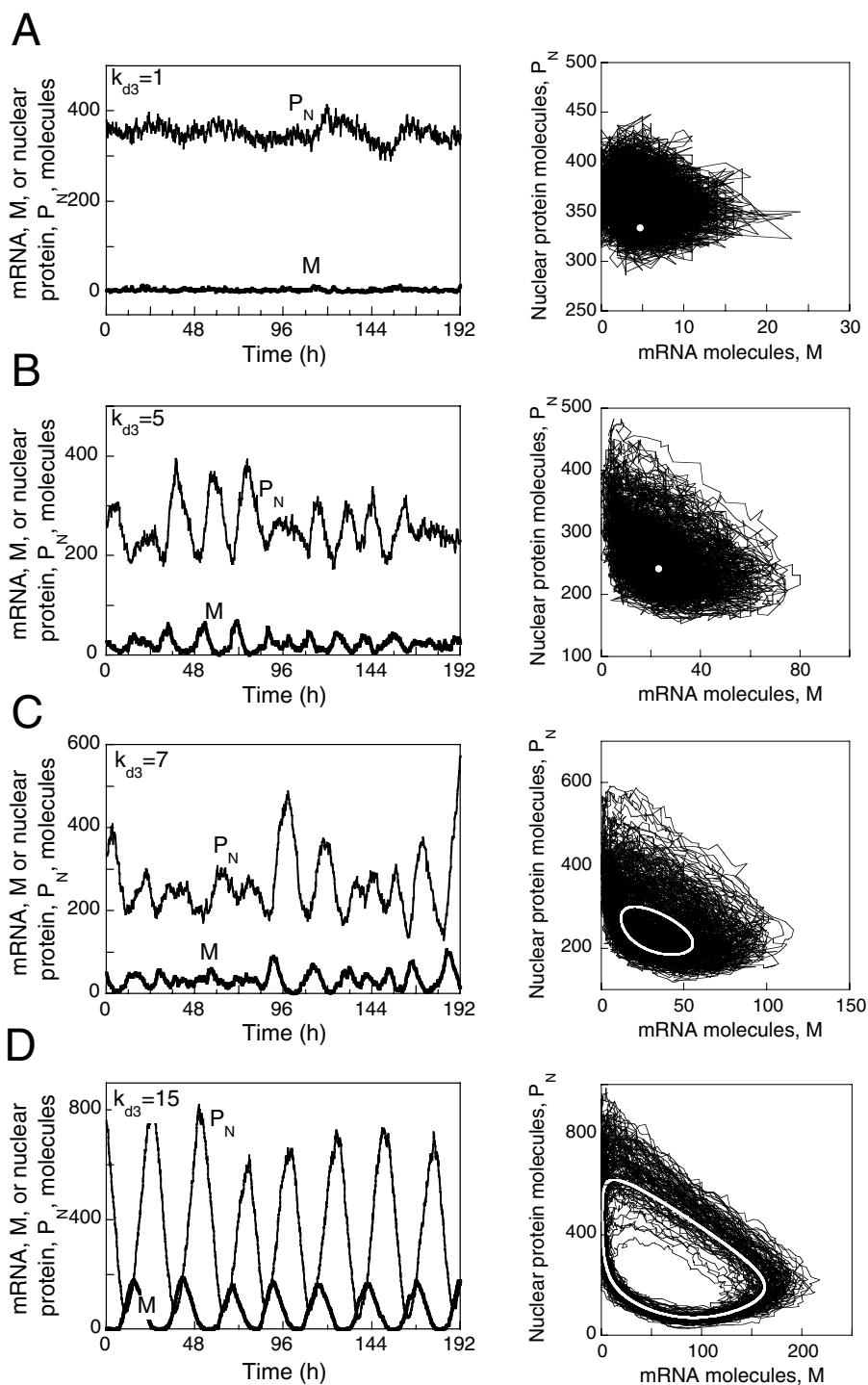


Figure 13.11. Effect of the proximity from a bifurcation point on the effect of molecular noise in the stochastic model for circadian rhythms. The different panels are established for the four increasing values of parameter k_{43} corresponding to the v_4 values shown in Figure 13.10: 0.1 (A), 0.5 (B), 0.7 (C) and 1.5 (d). The values of k_{43} listed in the left panels, are expressed here in molecules per h. The right-hand panels show the evolution in the phase plane, whereas the left-hand panels represent the corresponding temporal evolution of the number of *per* mRNA and nuclear PER molecules. (A) Fluctuations around a stable steady state. (B) Fluctuations around a stable steady state close to the bifurcation point. Damped oscillations occur in these conditions when the system is displaced from the stable steady state. In A and B, the white dot in the right-hand panel represents the stable steady state predicted by the deterministic version of the model in corresponding conditions. (C) Oscillations observed close to the bifurcation point. (D) Oscillations observed further from the bifurcation point, well into the domain of sustained oscillations. In C and D, the thick white curve in the right-hand panel represents the limit cycle predicted by the deterministic version of the model governed by Equations 13.1, in corresponding conditions. The smaller amplitude of the limit cycle in C as compared to the limit cycle in D is associated with an increased influence of molecular noise. The curves are obtained by means of the Gillespie algorithm applied to the model of Table 13.1 (Gonze et al. 2002a).



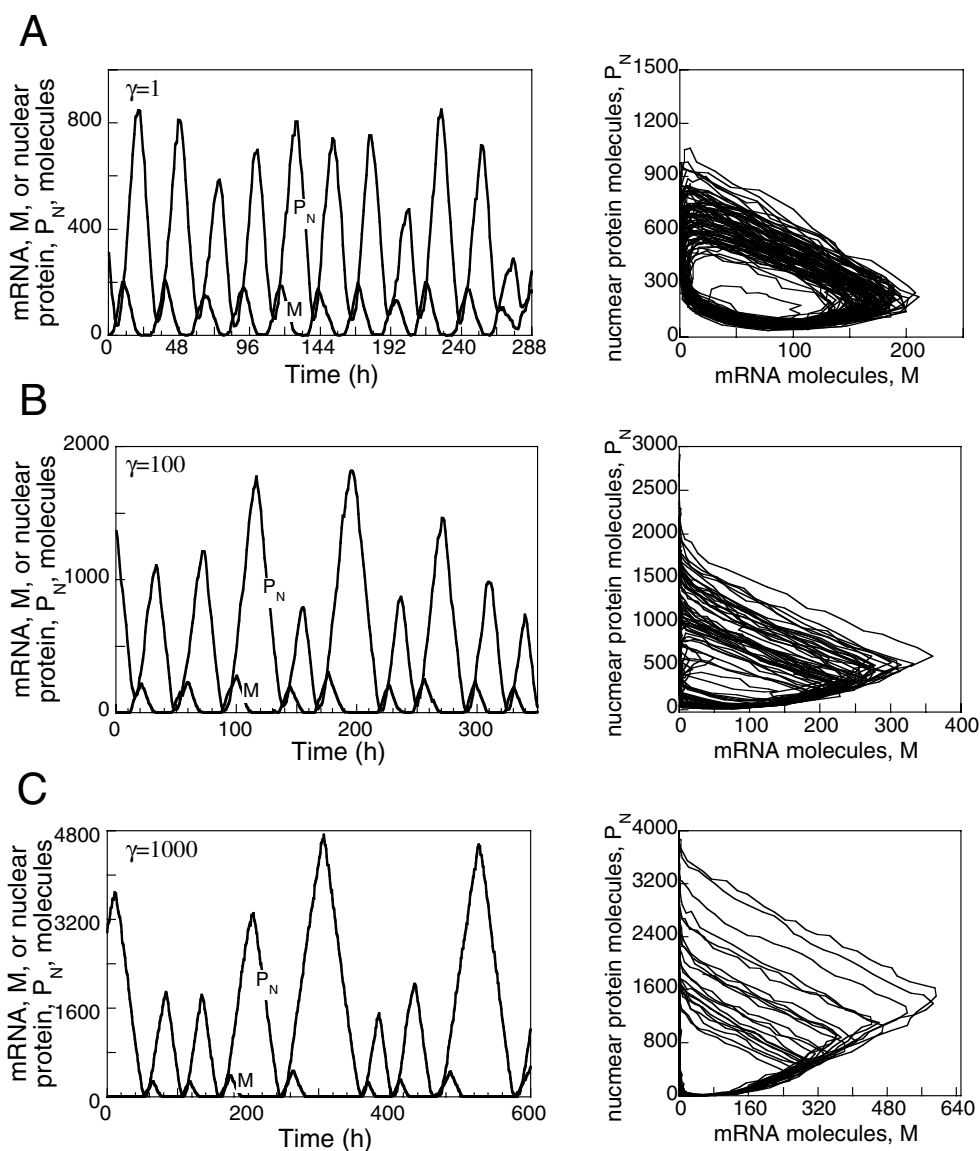


Figure 13.12. Irregular time series and trajectory in the phase space obtained by stochastic simulations of the core model for circadian rhythms for $\gamma = 1$ (a), $\gamma = 100$ (b), and $\gamma = 1,000$ (c). The curves were obtained for the model of Table 13.1, with $\Omega = 100$. Other parameter values are given in Table 13.2. The results should be compared with the bifurcation diagram established in Figure 13.13 as a function of γ for the corresponding fully developed version of the deterministic model. This diagram predicts that the steady state is stable and excitable for $\gamma = 100$ and 1,000, whereas sustained oscillations occur for $\gamma = 1$ when the steady state is unstable (Gonze et al. 2004a).

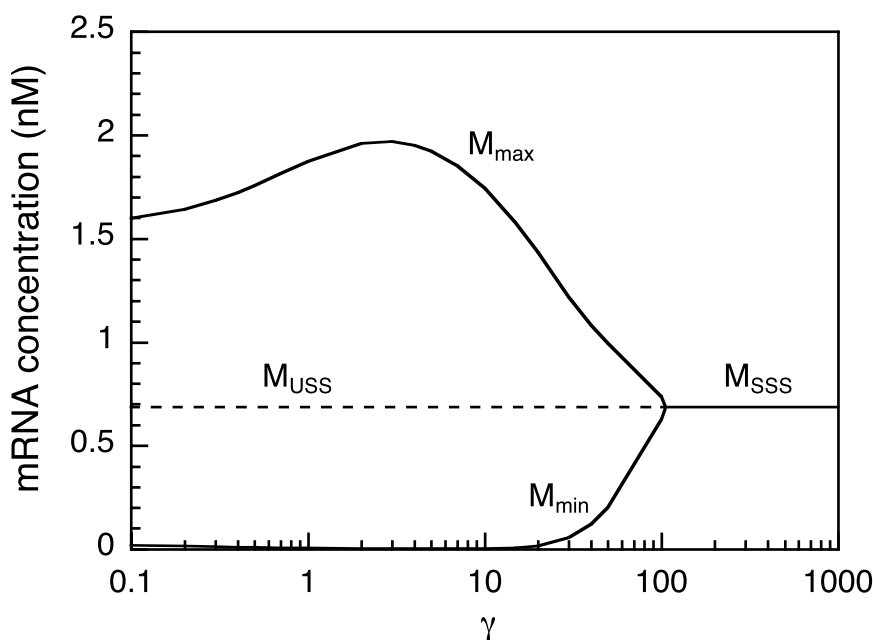


Figure 13.13. Bifurcation diagram showing the onset of circadian oscillations in the fully developed version of the deterministic core model, as a function of the scaling parameter γ . The latter parameter divides the association and dissociation rate constants a_i and d_i characterizing the binding of the repressor protein to the gene. The curve shows the steady-state level of mRNA, stable (solid line, M_{SSS}) or unstable (dashed line, M_{USS}), as well as the maximum (M_{max}) and minimum (M_{min}) mRNA concentration in the course of sustained oscillations. The diagram was determined by numerical integration of the 22 kinetic equations governing the dynamics of the fully developed deterministic model (Gonze et al. 2004a).

state. Numerical simulations performed with the 22-variable deterministic model for $\gamma = 1,000$, $\gamma = 100$, and $\gamma = 1$ show (Gonze et al. 2004a) that for $\gamma = 100$ the system still undergoes sustained low-amplitude oscillations. For $\gamma = 1,000$, the system evolves toward a stable steady state, as predicted by the bifurcation diagram of Figure 13.13, but this steady state is excitable: a small perturbation bringing the system slightly away from the steady state triggers a large excursion in the phase space, which corresponds to a burst of transcriptional activity, before the system returns to the stable steady state. This property of excitability also holds for the limit cycle observed for $\gamma = 100$. Thus, it is also possible to trigger large-amplitude peaks in gene transcription starting from such small-amplitude oscillations.

These results explain why oscillations predicted by stochastic simulations become highly irregular when the rate constants a_i and d_i decrease below a critical value. As shown by the study of the corresponding detailed deterministic model, such irregular oscillations reflect repetitive noise-induced large excursions away from a stable excitable steady state or from a small-amplitude limit cycle close to

the bifurcation point. The values of the bimolecular rate constants a_i used by Barkai and Leibler (2000) for simulating the circadian models of Figures 13.1a and 13.1b were probably below the critical value corresponding to sustained oscillations, which may explain their failure to obtain robust circadian oscillations in these models. When γ decreases (i.e., when the values of parameters a_i and d_i increase)—as in the case considered in Figure 13.8, which corresponds to $\gamma = 1$ —the oscillations become more regular and more robust, because the system operates well into the domain of sustained large-amplitude oscillations. The high values of parameters a_i and d_i corresponding to $\gamma = 1$ are of the order of those determined experimentally (Gonze et al. 2002b).

D. Non-developed stochastic models for circadian rhythms

The nonlinear terms appearing in the kinetic Equations 13.1 of the deterministic core model do not correspond to single reaction steps. These terms rather represent compact kinetic expressions obtained after application of quasi-steady-state hypotheses on enzyme-substrate or gene-repressor complexes. The resulting expressions are of the Michaelis—Menten type for enzyme reaction rates, or of the Hill type for cooperative binding of the repressor to the gene promoter. In the fully developed stochastic version of the core model, all reactions were decomposed into elementary steps (see Table 13.1).

Alternatively, we may resort to a simpler approach in which we attribute to each linear or nonlinear term of the kinetic equations a probability of occurrence of the corresponding reaction step (Gonze et al. 2002a). Then, in contrast to the treatment presented previously for the fully developed stochastic version we do not decompose the binding of the repressor P_N to the gene promoter into successive elementary steps, and rather retain the Hill function description for cooperative repression. A similar approach is taken for describing degradation of mRNA; translation of mRNA into protein, phosphorylation, or dephosphorylation reactions; and enzymatic degradation of fully phosphorylated clock protein and its reversible transport into and out of the nucleus. Some of these steps are of the Michaelian type, whereas others correspond to linear kinetics.

The comparison of stochastic simulations performed with the fully developed and non-developed versions of the core model showed that the two versions yield largely similar results (Gonze et al. 2002a). On the basis of these findings, a non-developed stochastic version of the 10-variable deterministic model governed by Equations 13.2, incorporating the formation of the PER-TIM complex, was considered. This version corresponds to a set of 30 reaction steps (listed in Table 13.3). Stochastic simulations show how sustained oscillations occur in this model under conditions corresponding to continuous darkness. As for the core model considered previously, the robustness of the oscillations is enhanced when the number of protein and mRNA molecules increases.

A conspicuous property of the 10-variable deterministic PER-TIM model for circadian rhythms in *Drosophila* is that it can produce autonomous chaotic behavior

Table 13.3. Nondeveloped stochastic version of the PER-TIM model for circadian rhythms [Gonze et al. 2003].

Reaction Number	Reaction Step	Probability of Reaction
1	$\xrightarrow{V_{sP}} M_P$	$w_1 = (v_{sP} \times \Omega) \frac{(K_{IP} \times \Omega)^n}{(K_{IP} \times \Omega)^n + C_N^n}$
2	$M_P \xrightarrow{V_{mP}} \rightarrow$	$w_2 = (v_{mP} \times \Omega) \frac{M_P}{(K_{mP} \times \Omega) + M_P}$
3	$M_P \xrightarrow{k_{sP}} M_P + P_0$	$w_3 = k_{sP} \times M_P$
4	$P_0 \xrightarrow{V_{IP}} P_1$	$w_4 = (V_{IP} \times \Omega) \frac{P_0}{(K_{IP} \times \Omega) + P_0}$
5	$P_1 \xrightarrow{V_{2P}} P_0$	$w_5 = (V_{2P} \times \Omega) \frac{P_1}{(K_{2P} \times \Omega) + P_1}$
6	$P_1 \xrightarrow{V_{3P}} P_2$	$w_6 = (V_{3P} \times \Omega) \frac{P_1}{(K_{3P} \times \Omega) + P_1}$
7	$P_2 \xrightarrow{V_{4P}} P_1$	$w_7 = (V_{4P} \times \Omega) \frac{P_2}{(K_{4P} \times \Omega) + P_2}$
8	$P_2 + T_2 \xrightarrow{k_3} C$	$w_8 = k_3 \times P_2 \times T_2 / \Omega$
9	$C \xrightarrow{k_4} P_2 + T_2$	$w_9 = k_4 \times C$
10	$P_2 \xrightarrow{V_{dP}} \rightarrow$	$w_{10} = (V_{dP} \times \Omega) \frac{P_2}{(K_{dP} \times \Omega) + P_2}$
11	$\xrightarrow{V_{dT}} M_T$	$w_{11} = (V_{dT} \times \Omega) \frac{(K_{IT} \times \Omega)^n}{(K_{IT} \times \Omega)^n + C_N^n}$
12	$M_T \xrightarrow{V_{mT}} \rightarrow$	$w_{12} = (V_{mT} \times \Omega) \frac{M_T}{(K_{mT} \times \Omega) + M_T}$
13	$M_T \xrightarrow{k_{sT}} M_T + T_0$	$w_{13} = k_{sT} \times M_T$
14	$T_0 \xrightarrow{V_{IT}} T_1$	$w_{14} = (V_{IT} \times \Omega) \frac{T_0}{(K_{IT} \times \Omega) + T_0}$
15	$T_1 \xrightarrow{V_{2T}} T_0$	$w_{15} = (V_{2T} \times \Omega) \frac{T_1}{(K_{2T} \times \Omega) + T_1}$
16	$T_1 \xrightarrow{V_{3T}} T_2$	$w_{16} = (V_{3T} \times \Omega) \frac{T_1}{(K_{3T} \times \Omega) + T_1}$
17	$T_2 \xrightarrow{V_{4T}} T_1$	$w_{17} = (V_{4T} \times \Omega) \frac{T_2}{(K_{4T} \times \Omega) + T_2}$
18	$T_2 \xrightarrow{V_{dT}} \rightarrow$	$w_{18} = (V_{dT} \times \Omega) \frac{T_2}{(K_{dT} \times \Omega) + T_2}$

Continues

Table 13.3. Nondeveloped stochastic version of the PER-TIM model for circadian rhythms [Gonze et al. 2003].—cont'd

Reaction Number	Reaction Step	Probability of Reaction
19	$C \xrightarrow{k_1} C_N$	$w_{19} = k_1 \times C$
20	$C_N \xrightarrow{k_2} C$	$w_{20} = k_2 \times C_N$
21	$M_P \xrightarrow{k_d} \rightarrow$	$w_{21} = k_d \times M_P$
22	$P_0 \xrightarrow{k_d} \rightarrow$	$w_{22} = k_d \times P_0$
23	$P_1 \xrightarrow{k_d} \rightarrow$	$w_{23} = k_d \times P_1$
24	$P_2 \xrightarrow{k_d} \rightarrow$	$w_{24} = k_d \times P_2$
25	$M_T \xrightarrow{k_d} \rightarrow$	$w_{25} = k_d \times M_T$
26	$T_0 \xrightarrow{k_d} \rightarrow$	$w_{26} = k_d \times T_0$
27	$T_1 \xrightarrow{k_d} \rightarrow$	$w_{27} = k_d \times T_1$
28	$T_2 \xrightarrow{k_d} \rightarrow$	$w_{28} = k_d \times T_2$
29	$C \xrightarrow{k_{dC}} \rightarrow$	$w_{29} = k_{dC} \times C$
30	$C_N \xrightarrow{k_{dN}} \rightarrow$	$w_{30} = k_{dN} \times C_N$

in a restricted domain in parameter space (see Section II.C). It was therefore interesting to check whether stochastic simulations were capable of reproducing this mode of dynamic behavior, which corresponds to the evolution to a strange attractor in the phase space. As shown in Figure 13.14, the strange attractor obtained by numerical integration of the deterministic Equations 13.2 can be recovered in corresponding conditions by simulations of the non-developed version of the stochastic model of Table 13.3. Here again, as illustrated in Figure 13.14, the larger the number of molecules of mRNAs and proteins involved in the oscillatory mechanism the closer the noisy stochastic trajectory is from the deterministic chaotic attractor.

The results obtained with stochastic models help to clarify the limits of validity of deterministic models for circadian oscillations. It appears that the deterministic approach provides a faithful picture as long as the number of molecules involved in the oscillatory mechanism exceeds a few tens or hundreds of molecules. Above this range, the larger the number of molecules the closer the stochastic trajectory from that predicted by the deterministic model.

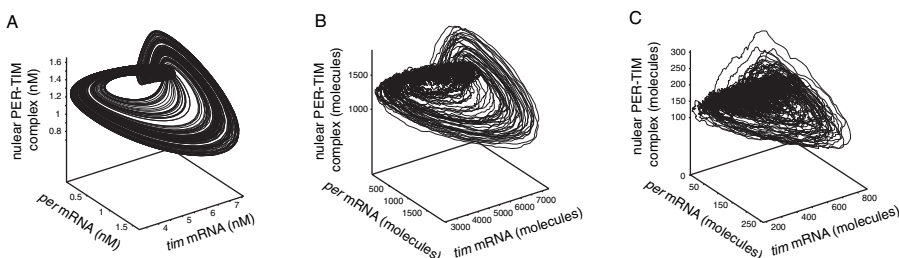


Figure 13.14. Effect of molecular noise on autonomous chaos. (a) Strange attractor corresponding to chaotic oscillations in the deterministic PER-TIM model for circadian rhythms. (b and c) Progressive dissolution of the strange attractor in the presence of molecular noise, for $\Omega = 1,000$ and 100 , respectively. The curve in a is obtained by numerical integration of Equations 13.2. In b and c, the curves are obtained by means of the Gillespie algorithm applied to the non-developed stochastic version of the PER-TIM model listed in Table 13.3 (Gonze et al. 2003).

IV. MODELING THE MAMMALIAN CIRCADIAN CLOCK

The molecular mechanism of circadian rhythms in mammals resembles that brought to light for *Drosophila*. In this organism, the negative feedback exerted by the PER-TIM complex is of an indirect rather than direct nature (Glossop et al. 1999). Thus, the transcription of the *per* and *tim* genes is triggered by a complex formed by the activators CYC and CLOCK. Binding of the PER-TIM complex to CYC and CLOCK prevents the activation of *per* and *tim* expression (Lee et al. 1999). In mammals the situation resembles that observed in *Drosophila*, but it is the CRY protein that forms a regulatory complex with a PER protein (Shearman et al. 2000; Reppert and Weaver 2002). Several forms of these proteins exist (PER1, PER2, PER3, CRY1, and CRY2). The complex CLOCK—BMAL1, formed by the products of the *Clock* and *Bmal1* genes, activates *Per* and *Cry* transcription. As in *Drosophila*, the PER-CRY complex inhibits the expression of the *Per* and *Cry* genes in an indirect manner, by binding to the complex CLOCK—BMAL1 (Lee et al. 2001; Reppert and Weaver 2002).

The mechanism of circadian rhythms in *Drosophila* and mammals thus relies on interlocked negative and positive feedback loops. In addition to the negative regulation of gene expression described previously, indirect positive regulation is involved. In *Drosophila*, the PER-TIM complex de-represses the transcription of *Clock* by binding to CLOCK, which exerts a negative autoregulation on the expression of its gene (Bae et al. 1998) via the product of the *vri* gene (Blau and Young 1999). In mammals, likewise, *Bmal1* expression is subjected to negative autoregulation by BMAL1, via the product of the *Rev-Erba* gene (Preitner et al. 2002). The PER-CRY complex enhances *Bmal1* expression in an indirect manner (Reppert and Weaver 2002) by binding to CLOCK—BMAL1 and thereby decreasing the transcription of the *Rev-Erba* gene (Preitner et al. 2002).

Models based on intertwined positive and negative regulatory loops have been proposed for *Drosophila* (Smolen et al. 2001; Ueda et al. 2001) and mammals (Forger and Peskin 2003, 2005; Leloup and Goldbeter 2003, 2004; Becker-Weimann et al. 2004). We shall focus here on the model proposed for the mammalian circadian clock, as it allows us to address the molecular dynamical bases of disorders of the human sleep/wake cycle associated with dysfunctions of the circadian clock.

A. Toward a detailed computational model for the mammalian circadian clock

The model for the mammalian circadian clock is schematized in Figure 13.15, both in a compact (a) and in a detailed manner (b). It describes the regulatory interactions between the products of the *Per*, *Cry*, *Bmal1*, and *Clock* genes. For simplicity, we do not distinguish between the *Per1*, *Per2*, and *Per3* genes and represent them in the model by a single *Per* gene. Similarly, *Cry1* and *Cry2* are represented by a single *Cry* gene. Moreover, as the *Clock* mRNA and its product (the CLOCK protein) are constitutively high in comparison to *Bmal1* mRNA and BMAL1 protein, they are considered in the model as parameters rather than variables.

We shall treat the regulatory effect of BMAL1 on *Bmal1* expression as a direct negative autoregulation. We have shown (Leloup and Goldbeter 2003) that similar conclusions are reached in an extended model in which the action of the REV-ERB α protein in the indirect negative feedback exerted by BMAL1 on the expression of its gene is considered explicitly. The version of the model without REV-ERB α is governed by a set of 16 kinetic equations (Leloup and Goldbeter 2003, 2004), whereas three more equations are needed in the extended model that incorporates the Rev-Erb α mRNA and the Rev-Erb α protein (Leloup and Goldbeter 2003).

In a certain range of parameter values, the 16- or 19-variable model for the mammalian clock produces sustained oscillations with a circadian period. These oscillations are endogenous, in that they occur for parameter values that remain constant in time, in agreement with the observation that circadian rhythms persist in continuous darkness or light. As observed experimentally (Lee et al. 2001; Reppert and Weaver 2002), *Bmal1* mRNA oscillates in antiphase with *Per* and *Cry* mRNAs (Figure 13.16a). The proteins also undergo antiphase oscillations and follow their mRNAs by a few hours (Figure 13.16b). Because most parameter values remain to be determined experimentally—as for the case of *Drosophila* (see Figures 13.2 and 13.3)—these oscillations were obtained for a semi-arbitrary choice of parameter values in a physiological range so as to yield a period of oscillations in continuous darkness (DD) close to 24 h.

To probe for entrainment of the circadian clock by LD cycles, we must incorporate the effect of light on *Per* expression. In continuous darkness, the maximum rate of *Per* expression, v_{sP} , remains at a low constant value. In LD, this rate varies periodically (e.g., as a square wave, going from a constant low value during the dark phase up to a higher constant value $v_{sP\max}$ during the light phase). In such conditions, entrainment by a 12 : 12 LD cycle (12 h of light followed by 12 h of darkness) can be obtained over an appropriate range of $v_{sP\max}$ values (Leloup and Goldbeter 2003).

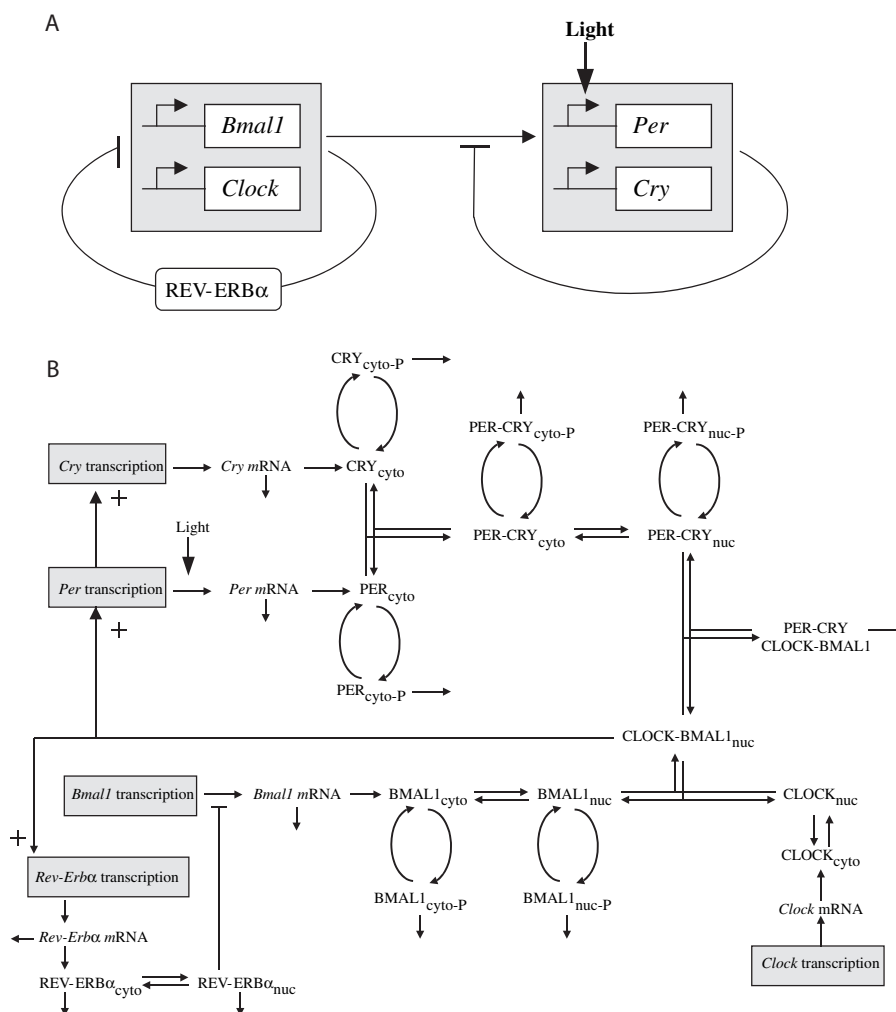


Figure 13.15. Model for the mammalian circadian clock involving interlocked negative and positive regulations of the *Per*, *Cry*, and *Bmal1* genes by their protein products. (a) Synthetic scheme of the model with the positive limb involving BMAL1-CLOCK and the negative limb involving PER-CRY. (b) Developed model for the mammalian clock (Leloup and Goldbeter 2003). The effect of light is to increase the rate of expression of the *Per* gene.

Interestingly, the phase of oscillations entrained in LD is particularly sensitive to changes in parameters that control the level of CRY protein and *Cry* mRNA. This was shown for parameter K_{AC} (the equilibrium constant describing the activating effect of CLOCK—BMAL1 on *Cry* expression) and for parameter v_{mC} , which measures the maximum rate of degradation of *Cry* mRNA. An example of the latter situation is illustrated in Figure 13.16d, where the only difference with respect to

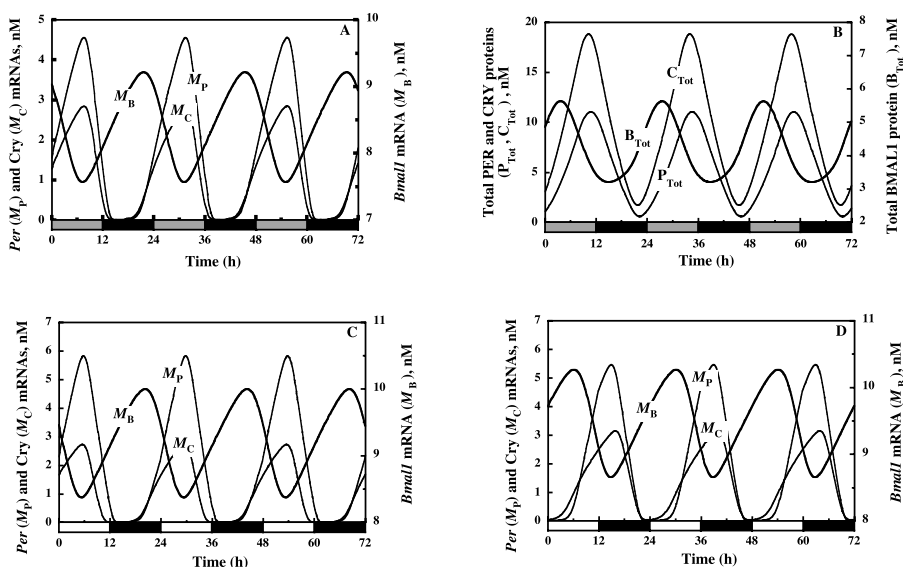


Figure 13.16. Circadian oscillations predicted by the mammalian clock model. (a) In constant darkness, the mRNA of *Bmal1* oscillates in antiphase with respect to the mRNAs of *Per* and *Cry*. (b) Corresponding protein oscillations in constant darkness. (c) Oscillations of the mRNAs after entrainment by 24-h light/dark (LD) cycles. The peak in *Per* mRNA occurs in the middle of the light phase. (d) Oscillations are delayed by 9 h and the peak in *Per* mRNA occurs in the dark phase when the value of parameter K_{AC} is decreased from 0.6 to 0.4 nM. Other parameter values correspond to the basal set of values listed in Table 1 in Leloup and Goldbeter (2003). In c and d, the maximum value of the rate of *Per* expression, v_{sp} , varies in a square-wave manner so that it remains at a constant low value of 1.5 nM/h during the 12-h-dark phase (black rectangle), and is raised up to the high value of 1.8 nM/h during the 12-h-light phase (white rectangle). The curves have been obtained by numerical integration of Equations 1 through 16 of the model without REV-ERB α (listed, together with parameter values, by Leloup and Goldbeter (2003)).

Figure 13.16c is a 10% change in parameter v_{mC} . The autonomous period in DD is 23.85 h and 23.70 h in Figures 13.16c and 13.16d, respectively, whereas the phase of *Per* mRNA is delayed by about 9 h in the latter case—so that *Per* mRNA reaches its maximum during the D phase instead of peaking in the L phase. This result is counterintuitive, in that we expect the maximum in *Per* mRNA to occur in phase L, because *Per* expression is enhanced by light. The virtue of the computational model is to alert us to the possibility that the phase of oscillations in LD may be highly labile, with the peak in *Per* mRNA shifting well into the D phase as a result of a small change in a light-insensitive parameter.

B. Multiple sources for oscillations in the circadian regulatory network

The genetic regulatory network underlying circadian rhythms contains intertwined positive and negative feedback loops. In view of the complexity of these regula-

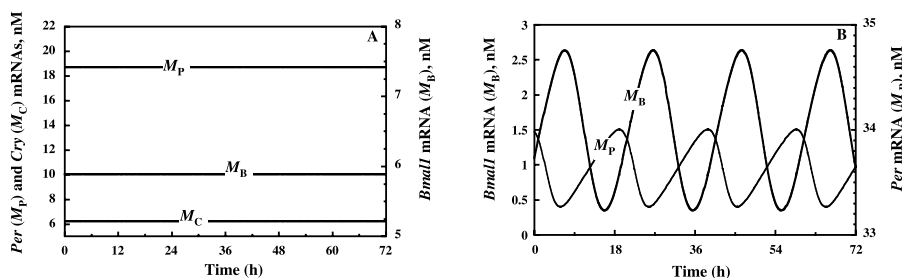


Figure 13.17. Multiple sources of oscillatory behavior in the genetic regulatory network controlling circadian rhythms. (a) Oscillations shown in Figures 13.16a and 13.16b disappear in the absence of PER protein synthesis ($k_{sp} = 0$). The curves show the asymptotic stable steady state reached after transients have subsided. (b) Sustained oscillations can nevertheless be restored when choosing a slightly different set of parameter values, even though $k_{sp} = 0$ (Leloup and Goldbeter 2003). The fact that oscillations can occur in the absence of PER protein indicates the existence of another oscillatory mechanism, which relies only on CLOCK-BMAL1 negative auto-regulation (see scheme in Figure 13.15a).

tory interactions, it should not be a surprise that more than one mechanism in the network may give rise to sustained oscillations. Evidence pointing to the existence of a second oscillatory mechanism (Leloup and Goldbeter 2003, 2004) stems from the fact that sustained oscillations generally disappear in the absence of PER protein (Figure 13.17a). However, even in such conditions sustained oscillations may occur with a period that is not necessarily circadian (Figure 13.17b). This second oscillator is based on the negative autoregulation exerted by BMAL1 on the expression of its gene, via the *Rev-Erb α* gene (see Figure 13.15).

Experimental observations so far suggest that if a second oscillator exists in the circadian regulatory network it does not manifest itself in producing rhythmic behavior. Thus, *mPer1/mPer2* (Zheng et al. 2001) or *mCry1/mCry2* (Van der Horst et al. 1999) double-knockout mice are arrhythmic. In some conditions, however, an extended light pulse can restore rhythmic behavior in a low proportion of *mPer1/mPer2* double-knockout mice (K. Bae and D. Weaver, personal communication).

In the absence of the negative feedback exerted by BMAL1 on the expression of its gene, oscillations can still originate from the PER—CRY negative feedback loop involving BMAL1. This result holds with the observation that circadian oscillations occur in the absence of REV-ERB α in mice (Preitner et al. 2002). Preventing altogether the synthesis of BMAL1 suppresses oscillations, because BMAL1 is involved in the mechanism of the two oscillators described previously.

C. Sensitivity analysis of the computational model for circadian rhythms

To assess the sensitivity of circadian oscillatory behavior to changes in parameter values, we determined for each parameter (one at a time) the range of values producing sustained oscillations (as well as the variation of the period over this range)

while keeping the other parameters set to their basal values (Leloup and Goldbeter, 2004; for an alternative sensitivity analysis, see Stelling et al. 2004). Such a sensitivity analysis was performed by constructing a series of bifurcation diagrams for four different sets of basal parameter values, each yielding circadian oscillations. Parameter set 1 was chosen so that oscillations disappear in the absence of PER protein or in the absence of negative autoregulation by BMAL1. Parameter set 2 corresponds to a situation in which oscillations can occur in the absence of PER, as a result of the negative autoregulation of BMAL1. Parameter set 3 corresponds to a situation in which circadian oscillations can occur in the absence of negative autoregulation by BMAL1. Finally, parameter set 4 was selected because oscillations can occur in the absence of PER or in the absence of negative autoregulation of BMAL1. On the basis of this analysis we may distinguish between two types of sensitivity: the first relates to the size of the oscillatory domain and the other to the influence on the period.

For some parameters the range of values producing sustained oscillations is quite narrow, less than one order of magnitude, whereas for other parameters it is much larger and extends over several orders of magnitude. The largest variation in period, by a factor close to 3, is observed for parameters that measure, respectively, the entry of the PER-CRY complex into the nucleus, and the formation of the inactive complex between PER-CRY and CLOCK-BMAL1 in the nucleus. For some sets of parameter values, the period may vary significantly (by a factor close to 2) over the oscillatory domain, whereas for other sets of parameter values the change in period as a function of this parameter may be reduced. Parameters for which the range of values yielding oscillations is narrowest are mainly those linked to BMAL1 and its mRNA. On the basis of these results, we may conclude that parameters affecting the level of BMAL1 possess the narrowest range of values producing sustained oscillations, whereas the period is most affected by the parameters measuring the entry of the PER-CRY complex into the nucleus and the formation of the inactive complex between PER-CRY and CLOCK-BMAL1.

D. From molecular mechanism to physiological disorders

The computational model for circadian oscillations in mammals provides us with the unique opportunity to address not only the molecular mechanism of a key biological rhythm but the dynamical bases of physiological disorders resulting from perturbations of the human circadian clock. Several disorders of the sleep/wake cycle are indeed associated with dysfunctions of the circadian clock in humans. In the familial advanced sleep/phase syndrome (FASPS), the phase of the sleep/wake cycle in LD is advanced by several hours, as a result of a decreased rate of PER phosphorylation (Toh et al. 2001). In a family in which FASPS is present over five generations, those affected by the syndrome tend to go to sleep around 7:30 p.m. and awake around 4:30 a.m. Moreover, in a patient affected by FASPS the period of the circadian clock in DD was reduced down to 23.5 h from a normal mean value of 24.4 h (Jones et al. 1999).

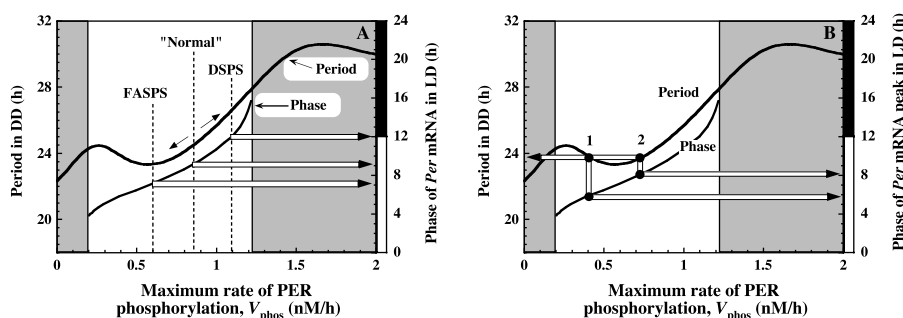


Figure 13.18. Relating the mammalian clock model to syndromes associated with disorders of the sleep/wake cycle in humans (Leloup and Goldbeter 2003). (a) Effect of the maximum rate of PER phosphorylation on the free running period in DD and on the phase of the oscillations in LD. The phase corresponds to the time (in h) at which the maximum in *Per* mRNA occurs after the onset of the L phase. Decreasing (increasing) the rate of phosphorylation of the PER protein, V_{phos} , with respect to the “normal” situation can produce a phase advance (delay) as well as a decrease (increase) in free running period that accounts for the phase shift observed in the familial advanced sleep phase syndrome (FASPS) or the delayed sleep phase syndrome (DSPS). (b) Situations 1 and 2 show that different values of the control parameter can produce different phases after entrainment, even though they correspond to the same free running period in DD. The gray areas on the left and right in the two panels refer to absence of entrainment (see Figure 13.19).

The phase advance characteristic of FASPS can be accounted for by the model as a result of a decrease in parameter V_{phos} , which measures the maximum rate of PER phosphorylation by the protein kinase CK1 ϵ . As in clinical observations (Jones et al. 1999), the advance of the phase in LD then accompanies a decrease in autonomous period as the phosphorylation rate decreases (Leloup and Goldbeter 2003). Such a decrease in period in DD can be observed over parts of the bifurcation diagram established as a function of V_{phos} (see Figure 13.18a). The model could be used similarly to address the delayed sleep phase syndrome, which is the mirror physiological disorder of the sleep/wake cycle and appears to be associated with increased rate of PER phosphorylation (Ebisawa et al. 2001; Archer et al. 2003). The bifurcation diagram of Figure 13.18a indicates that an increase in V_{phos} may correspond to a delayed phase of the sleep/wake cycle in LD, and to an increase in the autonomous period of circadian oscillations in DD. An interesting prediction arising from Figure 13.18b is that two distinct values of V_{phos} may yield the same period in DD and different phases upon entrainment in LD.

For a long time the model for the mammalian circadian clock placed us in a quandary, as the model failed to account for the most conspicuous property of circadian rhythms; namely, their entrainment by LD cycles. There is generally a range of parameter values in which entrainment occurs, but we failed to find any such range when the light-sensitive parameter (the maximum rate of *Per* expression) was made to vary in a square wave manner. Regardless of the magnitude of the periodic variation, entrainment did not occur. We then realized that the level of CRY

protein was critical for entrainment by LD cycles. When the level of CRY remains too low, free PER builds up during successive light phases, as there is not enough CRY with which to form a complex. Consequently, entrainment fails to occur (Leloup and Goldbeter 2003). It was sufficient to raise the level of CRY—by increasing the rate of PER synthesis or the rate of *Per* expression, or by decreasing the rate of degradation of either PER or *Per* mRNA—for entrainment to occur.

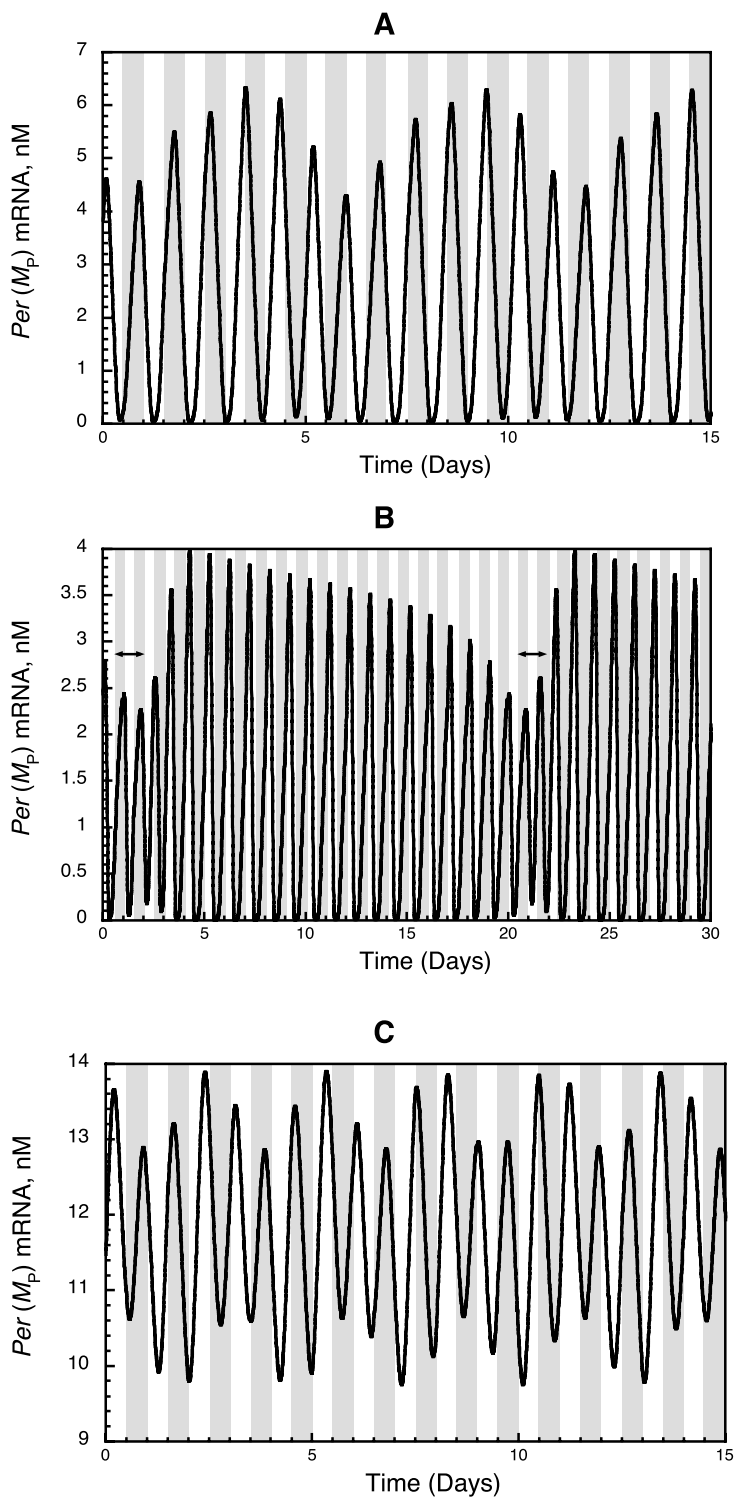
If entrainment failure is so easy to obtain in the model, could it be that a corresponding syndrome exists in human physiology? The answer is yes: there is a condition known as non-24-h sleep/wake syndrome (Richardson and Malin 1996), in which the time at which the subject goes to sleep is drifting every day. This slow drift is sometimes accompanied by “jumps” in the phase ϕ of the sleep/wake cycle in LD conditions. During such jumps, ϕ rapidly traverses one phase of the LD cycle in a few days, and slowly drifts across the other phase of the LD cycle during a much longer time (on the order of several weeks). The absence of entrainment in the model corresponds to quasi-periodic oscillations in LD. These oscillations can be associated or not with phase jumps, as shown in Figure 13.19 in panels A and B, respectively. Chaotic oscillations may also result from the periodic forcing by LD cycles (Figure 13.19c).

We are currently using the model to search for conditions other than decreased levels of CRY, which might also lead to the failure of entrainment in LD. If the non-24-h sleep/wake cycle syndrome is indeed due to altered levels of CRY, the results suggest that restoring adequate levels of the protein might allow entrainment to occur.

V. CONCLUSIONS

Remarkable advances have been made during the last two decades in unraveling the molecular bases of circadian rhythms—first in *Drosophila* and *Neurospora*, and more recently in cyanobacteria, plants, and mammals. Based on experimentally determined mechanisms, computational models of increasing complexity have been proposed for these rhythms. As reviewed in this chapter, computational approaches throw light on the precise conditions in which circadian oscillations occur as a result of genetic regulation. The models also account for a variety of

Figure 13.19. Absence of entrainment and the non-24-h sleep/wake cycle syndrome. The phase of the circadian oscillations does not always lock to a constant value with respect to the 24-h LD cycle, in contrast to what occurs in the case of entrainment. Lack of entrainment can lead to quasi-periodic behavior (a), which is sometimes accompanied by phase jumps (b) corresponding to slow drifts of the phase followed by rapid progression through the L or D phase (horizontal arrows). Chaotic behavior (c) can also be observed as a result of forcing by the LD cycle. Gray and white columns represent the D and L phases of the LD cycles, respectively. Parameter values are as in Table 1 of Leloup and Goldbeter (2003), with $v_{mP} = 0.95 \text{ nMh}^{-1}$ (a), 1.45 nMh^{-1} (b), or 0.70 nMh^{-1} (c).



properties of circadian rhythms, such as phase shifting or long-term suppression by light pulses, entrainment by light/dark cycles, and temperature compensation.

When the numbers of molecules of protein or mRNA involved in the oscillatory mechanism are very low, it becomes necessary to resort to stochastic approaches. We have shown by means of stochastic simulations that coherent sustained oscillations emerge from molecular noise in the genetic regulatory network as soon as the maximum numbers of mRNA and clock protein molecules are in the tens and hundreds, respectively. At higher numbers of molecules, the stochastic models yield results that are largely similar to the predictions of the corresponding deterministic models. The latter therefore provide a useful representation of circadian oscillatory behavior over a wide range of conditions.

Among the factors that contribute to the robustness of circadian rhythms with respect to molecular noise are the degree of cooperativity of repression, the distance from a bifurcation point, and the rate constants measuring the binding of the repressor to the gene. All models considered here pertain to the onset of circadian rhythms at the cellular level. The intercellular coupling of oscillatory cells—for example, in the suprachiasmatic nuclei (SCN), which represent the central circadian pacemaker in mammals (Kunz and Achermann 2003; Gonze et al. 2005)—may further contribute to the robustness of circadian rhythms.

The computational approach supports the view (Reppert and Weaver 2002) that the genetic regulatory mechanism of sustained circadian oscillations is similar in both the central and peripheral (Schibler et al. 2003; Yoo et al. 2004) oscillators, and that the observed differences in phase are of a quantitative rather than qualitative nature.

We have used the case of circadian rhythms to show how more and more complex computational models must be considered to accommodate the accelerating flux of new experimental observations. A question that arises naturally is whether such an ever-increasing complexity of the models is really needed. It appears that as with geographical maps a balance must be made between the necessity of including the most relevant details and the desire to not become lost in a too meticulous description, because the model might quickly become so complex that its detailed numerical study would become highly cumbersome.

An example of molecular detail that has to be incorporated is the phosphorylation of the PER protein: even if sustained oscillations are possible, in principle, in the absence of PER covalent modification the phosphorylation step is needed not only to account for the effect of mutations in the protein kinase that phosphorylates PER but also to account for some disorders of the sleep/wake cycle in humans related to altered PER phosphorylation. Moreover, as described in this chapter, several results can only be obtained in models that possess a minimum degree of complexity. Thus, autonomous chaos was obtained in the 10-variable model for circadian rhythms in *Drosophila* incorporating the formation of a PER-TIM complex, but not in the five-variable model based on PER alone. In the mammalian clock model, incorporation of additional feedback loops brought to light the possibility of multiple sources of oscillatory behavior.

Finally, circadian rhythms provide a case in point for showing how computational models can be used to address a wide range of issues, extending from molecular mechanism to physiological disorders. Identifying the origin of dysfunctions and predicting ways of obviating them in metabolic or genetic regulatory networks on the basis of numerical simulations presents a key challenge for computational biology.

ACKNOWLEDGMENTS

This work was supported by grants 3.4607.99 and 3.4636.04 from the Fonds de la Recherche Scientifique Médicale (F.R.S.M., Belgium), DARPA-AFRL grant F30602-02-0554, and the BIOSIM Network of Excellence within the FP6 Program of the European Union. J.-C. L. and D. G. are, respectively, Chercheur qualifié and Chargé de recherches du Fonds National de la Recherche Scientifique (F.N.R.S., Belgium). This chapter was prepared while A. G. held a Chaire Internationale de Recherche Blaise Pascal de l'Etat et de la Région d'Ile-de-France, gérée par la Fondation de l'Ecole Normale Supérieure at the University of Paris Sud-Orsay (France), in the Institute of Genetics and Microbiology directed by Professor Michel Jacquet, whose hospitality is gratefully acknowledged.

REFERENCES

- Alabadi, D., Oyama, T., Yanovsky, M. J., Harmon, F. G., Mas, P., and Kay, S. A. (2001). Reciprocal regulation between TOC1 and LHY/CCA1 within the Arabidopsis circadian clock. *Science* **293**:880–883.
- Archer, S. N., Robilliard, D. L., Skene, D. J., Smits, M., Williams, A., Arendt, J., and von Schantz, M. (2003). A length polymorphism in the circadian clock gene *Per3* is linked to delayed sleep phase syndrome and extreme diurnal preference. *Sleep* **26**:413–415.
- Arkin, A., Ross, J., and McAdams, H. H. (1998). Stochastic kinetic analysis of developmental pathway bifurcation in phage lambda-infected *Escherichia coli* cells. *Genetics* **149**:1633–1648.
- Aronson, B. D., Johnson, K. A., Loros, J. J., and Dunlap, J. C. (1994). Negative feedback defining a circadian clock: Autoregulation of the clock gene frequency. *Science* **263**:1578–1584.
- Bae, K., Lee, C., Sidote, D., Chuang, K.-Y., and Edery, I. (1998). Circadian regulation of a *Drosophila* homolog of the mammalian *Clock* gene: PER and TIM function as positive regulators. *Mol. Cell. Biol.* **18**:6142–6151.
- Baras, F. (1997). Stochastic analysis of limit cycle behaviour. In *Stochastic Dynamics: Lecture Notes in Physics* (L. Schimansky-Geier and T. Poeschel eds.), pp. 167–178, Berlin: Springer.
- Baras, F., Pearson, J. E., and Mansour, M. M. (1990). Microscopic simulation of chemical oscillations inhomogeneous systems. *J. Chem. Phys.* **93**:5747–5750.
- Barkai, N., and Leibler, S. (2000). Circadian clocks limited by noise. *Nature* **403**:267–268.

- Baylies, M. K., Weiner, L., Vossball, L. B., Saez, L., and Young, M. W. (1993). Genetic, molecular, and cellular studies of the *per* locus and its products in *Drosophila melanogaster*. In *Molecular Genetics of Biological Rhythms* (M. W. Young ed.), pp. 123–153, New-York: Marcel Dekker.
- Becker-Weimann, S., Wolf, J., Herzel, H., and Kramer, A. (2004). Modeling feedback loops of the mammalian circadian oscillator. *Biophys. J.* **87**:3023–3034.
- Blau, J., and Young, M. W. (1999). Cycling *vrille* expression is required for a functional *Drosophila* clock. *Cell* **99**:661–671.
- Busza, A., Emery-Le, M., Rosbash, M., and Emery, P. (2004). Roles of the two *Drosophila* CRYPTOCHROME structural domains in circadian photoreception. *Science* **304**:1503–1506.
- Darlington, T. K., Wager-Smith, K., Ceriani, M. F., Staknis, D., Gekakis, N., Steeves, T. D. L., Weitz, C. J., Takahashi, J. S., and Kay, S. A. (1998). Closing the circadian loop: CLOCK-induced transcription of its own inhibitors *per* and *tim*. *Science* **280**:1599–1603.
- Doedel, E. J. (1981). AUTO: A program for the automatic bifurcation analysis of autonomous systems. *Cong. Numer.* **30**:265–384.
- Dunlap, J. C. (1993). Genetic analysis of circadian clocks. *Annu. Rev. Physiol.* **55**:683–728.
- Dunlap, J. C. (1999). Molecular bases for circadian clocks. *Cell* **96**:271–290.
- Ebisawa, T., Uchiyama, M., Kajimura, N., Mishima, K., Kamei, Y., Katoh, M., Watanabe, T., Sekimoto, M., Shibui, K., Kim, K., et al. (2001). Association of structural polymorphisms in the human *period3* gene with delayed sleep phase syndrome. *EMBO Rep.* **2**:342–346.
- Ederly, I., Zwiebel, L. J., Dembinska, M. E., and Rosbash, M. (1994). Temporal phosphorylation of the *Drosophila* period protein. *Proc. Natl. Acad. Sci. USA* **91**:2260–2264.
- Forger, D. B., and Peskin, C. S. (2003). A detailed predictive model of the mammalian circadian clock. *Proc. Natl. Acad. Sci. USA* **100**:14806–14811.
- Forger, D. B., and Peskin, C. S. (2005). Stochastic simulation of the mammalian circadian clock. *Proc. Natl. Acad. Sci. USA* **102**:321–324.
- Gillespie, D. T. (1976). A general method for numerically simulating the stochastic time evolution of coupled chemical reactions. *J. Comput. Phys.* **22**:403–434.
- Gillespie, D. T. (1977). Exact stochastic simulation of coupled chemical reactions. *J. Phys. Chem.* **81**:2340–2361.
- Glossop, N. R. J., Lyons, L. C., and Hardin, P. E. (1999). Interlocked feedback loops within the *Drosophila* circadian oscillator. *Science* **286**:766–768.
- Goldbeter, A. (1995). A model for circadian oscillations in the *Drosophila* period protein (PER). *Proc. R. Soc. London Ser. B* **261**:319–324.
- Goldbeter, A. (1996). *Biochemical Oscillations and Cellular Rhythms: The Molecular Bases of Periodic and Chaotic Behavior*. Cambridge UK: Cambridge University Press.
- Gonze, D., and Goldbeter, A. (2000). Entrainment versus chaos in a model for a circadian oscillator driven by light-dark cycles. *J. Stat. Phys.* **101**:649–663.
- Gonze, D., Leloup, J.-C., and Goldbeter, A. (2000). Theoretical models for circadian rhythms in *Neurospora* and *Drosophila*. *C. R. Acad. Sci. III.* **323**(323):57–67.
- Gonze, D., Halloy, J., and Goldbeter, A. (2002a). Deterministic versus stochastic models for circadian rhythms. *J. Biol. Phys.* **28**:637–653.
- Gonze, D., Halloy, J., and Goldbeter, A. (2002b). Robustness of circadian rhythms with respect to molecular noise. *Proc. Natl. Acad. Sci. USA* **99**:673–678.
- Gonze, D., Roussel, M. R., and Goldbeter, A. (2002c). A Model for the enhancement of fitness in cyanobacteria based on resonance of a circadian oscillator with the external light-dark cycle. *J. Theor. Biol.* **214**:577–597.

- Gonze, D., Halloy, J., Leloup, J.-C., and Goldbeter, A. (2003). Stochastic models for circadian rhythms: Effect of molecular noise on periodic and chaotic behaviour. *C. R. Biologies* **326**:189–203.
- Gonze, D., Halloy, J., and Goldbeter, A. (2004a). Emergence of coherent oscillations in stochastic models for circadian rhythms. *Physica A*. **342**:221–233.
- Gonze, D., Halloy, J., and Goldbeter, A. (2004b). Stochastic models for circadian oscillations: Emergence of a biological rhythm. *Int. J. Quantum Chem.* **98**:228–238.
- Gonze, D., Bernard, S., Waltermann, C., Kramer, A., and Herzog, H. (2005). Spontaneous synchronization of coupled circadian oscillators. *Biophys. J.* **89**:120–129.
- Goodwin, B. C. (1965). Oscillatory behavior in enzymatic control processes. *Adv. Enzyme Regul.* **3**:425–438.
- Grima, B., Lamouroux, A., Chelot, E., Papin, C., Limbourg-Bouchon, B., and Rouyer, F. (2002). The F-box protein Slimb controls the levels of clock proteins Period and Timeless. *Nature* **420**:178–182.
- Hall, J. C., and Rosbash, M. (1988). Mutations and molecules influencing biological rhythms. *Annu. Rev. Neurosci.* **11**:373–393.
- Hardin, P. E., Hall, J. C., and Rosbash, M. (1990). Feedback of the *Drosophila* period gene product on circadian cycling of its messenger RNA levels. *Nature* **343**:536–540.
- Hardin, P. E., Hall, J. C., and Rosbash, M. (1992). Circadian oscillations in period gene mRNA levels are transcriptionally regulated. *Proc. Natl. Acad. Sci. USA* **89**:11711–11715.
- Hunter-Ensor, M., Ousley, A., and Sehgal, A. (1996). Regulation of the *Drosophila* protein timeless suggests a mechanism for resetting the circadian clock by light. *Cell* **84**:677–685.
- Jewett, M. E., and Kronauer, R. E. (1998). Refinement of a limit cycle oscillator model of the effects of light on the human circadian pacemaker. *J. Theor. Biol.* **192**:455–465.
- Jones, C. R., Campbell, S. S., Zane, S. E., Cooper, F., DeSano, A., Murphy, P. J., Jones, B., Czajkowski, L., and Ptacek, L. J. (1999). Familial advanced sleep-phase syndrome: A short-period circadian rhythm variant in humans. *Nat. Med.* **5**:1062–1065.
- Ko, H. W., Jiang, J., and Edery, I. (2002). Role for Slimb in the degradation of *Drosophila* Period protein phosphorylated by Doubletime. *Nature* **420**:673–678.
- Konopka, R. J. (1979). Genetic dissection of the *Drosophila* circadian system. *Fed. Proc.* **38**:2602–2605.
- Konopka, R. J., and Benzer, S. (1971). Clock mutants of *Drosophila melanogaster*. *Proc. Natl. Acad. Sci. USA* **68**:2112–2116.
- Konopka, R. J., Pittendrigh, C., and Orr, D. (1989). Reciprocal behaviour associated with altered homeostasis and photosensitivity of *Drosophila* clock mutants. *J. Neurosci.* **6**:1–10.
- Kunz, H., and Achermann, P. (2003). Simulation of circadian rhythm generation in the suprachiasmatic nucleus with locally coupled self-sustained oscillators. *J. Theor. Biol.* **224**:63–78.
- Lee, C., Parikh, V., Itsukaichi, T., Bae, K., and Edery, I. (1996). Resetting the *Drosophila* clock by photic regulation of PER and a PER-TIM complex. *Science* **271**:1740–1744.
- Lee, C., Bae, K., and Edery, I. (1999). PER and TIM inhibit the DNA binding activity of a *Drosophila* CLOCK-CYC/dBMAL1 heterodimer without disrupting formation of the heterodimer: A basis for circadian transcription. *Mol. Cell. Biol.* **19**:5316–5325.
- Lee, K., Loros, J. J., and Dunlap, J. C. (2000). Interconnected feedback loops in the *Neurospora* circadian system. *Science* **289**:107–110.
- Lee, C., Etchegaray, J. P., Cagampang, F. R., Loudon, A. S., and Reppert, S. M. (2001). Post-translational mechanisms regulate the mammalian circadian clock. *Cell* **107**:855–867.

- Leloup, J.-C., and Goldbeter, A. (1997). Temperature compensation of circadian rhythms: Control of the period in a model for circadian oscillations of the PER protein in *Drosophila*. *Chronobiol. Int.* **14**:511–520.
- Leloup, J.-C., and Goldbeter, A. (1998). A model for circadian rhythms in *Drosophila* incorporating the formation of a complex between the PER and TIM proteins. *J. Biol. Rhythms* **13**:70–87.
- Leloup, J.-C., and Goldbeter, A. (1999). Chaos and birhythmicity in a model for circadian oscillations of the PER and TIM proteins in *Drosophila*. *J. Theor. Biol.* **198**:445–459.
- Leloup, J.-C., and Goldbeter, A. (2001). A molecular explanation for the long-term suppression of circadian rhythms by a single light pulse. *Am. J. Physiol. Regul. Integrat. Comp. Physiol.* **280**:R1206–R1212.
- Leloup, J.-C., and Goldbeter, A. (2003). Toward a detailed computational model for the mammalian circadian clock. *Proc. Natl. Acad. Sci. USA* **100**:7051–7056.
- Leloup, J.-C., and Goldbeter, A. (2004). Modeling the mammalian circadian clock: Sensitivity analysis and multiplicity of oscillatory mechanisms. *J. Theor. Biol.* **230**:541–562.
- Leloup, J.-C., Gonze, D., and Goldbeter, A. (1999). Limit cycle models for circadian rhythms based on transcriptional regulation in *Neurospora* and *Drosophila*. *J. Biol. Rhythms* **14**:433–448.
- McAdams, H. H., and Arkin, A. (1997). Stochastic mechanisms in gene expression. *Proc. Natl. Acad. Sci. USA* **94**:814–819.
- Morrow, M. W., Garceau, N. Y., and Dunlap, J. C. (1997). Dissection of a circadian oscillation into discrete domains. *Proc. Natl. Acad. Sci. USA* **94**:3877–3882.
- Moore-Ede, M. C., Sulzman, F. M., and Fuller, C. A. (1982). *The Clocks That Time Us: Physiology of the Circadian Timing System*. Cambridge, MA: Harvard University Press.
- Morton-Firth, C. J., and Bray, D. (1998). Predicting temporal fluctuations in an intracellular signalling pathway. *J. Theor. Biol.* **192**:117–128.
- Myers, M. P., Wager-Smith, K., Rothenfluh-Hilfiker, A., and Young, M. W. (1996). Light-induced degradation of TIMELESS and entrainment of the *Drosophila* circadian clock. *Science* **271**:1736–1740.
- Nicolis, G., and Prigogine, I. (1977). *Self-Organization in Nonequilibrium Systems: From Dissipative Structures to Order through Fluctuations*. New York: Wiley.
- Pittendrigh, C. S. (1960). Circadian rhythms and the circadian organization of living systems. *Cold Spring Harbor Symp. Quant. Biol.* **25**:159–184.
- Preitner, N., Damiola, F., Lopez-Molina, L., Zakany, J., Duboule, D., Albrecht, U., and Schibler, U. (2002). The orphan nuclear receptor REV-ERB α controls circadian transcription within the positive limb of the mammalian circadian oscillator. *Cell* **110**:251–260.
- Qiu, J., and Hardin, P. E. (1996). *per* mRNA cycling is locked to lights-off under photoperiodic conditions that support circadian feedback loop function. *Mol. Cell. Biol.* **16**:4182–4188.
- Reppert, S., and Weaver, D. (2002). Coordination of circadian timing in mammals. *Nature* **418**:935–941.
- Richardson, G. S., and Malin, H. V. (1996). Circadian rhythm sleep disorders: Pathophysiology and treatment. *J. Clin. Neurophysiol.* **13**:17–31.
- Ruoff, P., and Rensing, L. (1996). The temperature-compensated Goodwin model simulates many circadian clock properties. *J. Theor. Biol.* **179**:275–285.
- Ruoff, P., Vinsjevsk, M., Monnerjahn, C., and Rensing, L. (2001). The Goodwin model: Simulating the effect of light pulses on the circadian sporulation rhythm of *Neurospora crassa*. *J. Theor. Biol.* **209**:29–42.

- Rutula, J. E., Suri, V., Le, M., So, W. V., Rosbash, M., and Hall, J. C. (1998). CYCLE is a second bHLH-PAS clock protein essential for circadian rhythmicity and transcription of *Drosophila period* and *timeless*. *Cell* **93**:805–814.
- Sassone-Corsi, P. (1994). Rhythmic transcription and autoregulatory loops: Winding up the biological clock. *Cell* **78**:361–364.
- Schibler, U., Ripperger, J., and Brown, S. A. (2003). Peripheral circadian oscillators in mammals: Time and food. *J. Biol. Rhythms* **18**:250–260.
- Shearman, L. P., Sriram, S., Weaver, D. R., Maywood, E. S., Chaves, I., Zheng, B., Kume, K., Lee, C. C., van der Horst, G. T., Hastings, M. H., and Reppert, S. M. (2000). Interacting molecular loops in the mammalian circadian clock. *Science* **288**:1013–1019.
- Smolen, P., Baxter, D. A., and Byrne, J. H. (2001). Modeling circadian oscillations with interlocking positive and negative feedback loops. *J. Neurosci.* **21**:6644–6656.
- Stelling, J., Gilles, E. D., and Doyle, F. J. 3rd (2004). Robustness properties of circadian clock architectures. *Proc. Natl. Acad. Sci. USA* **101**:13210–13215.
- Takahashi, J. S. (1992). Circadian clock genes are ticking. *Science* **258**:238–240.
- Toh, K. L., Jones, C. R., He, Y., Eide, E. J., Hinz, W. A., Virshup, D. M., Ptacek, L. J., and Fu, Y.-H. (2001). An *hPer2* phosphorylation site mutation in familial advanced sleep-phase syndrome. *Science* **291**:1040–1043.
- Ueda, H. R., Hagiwara, M., and Kitano, H. (2001). Robust oscillations within the interlocked feedback model of *Drosophila* circadian rhythm. *J. Theor. Biol.* **210**:401–406.
- van der Horst, G. T., Muijtjens, M., Kobayashi, K., Takano, R., Kanno, S., Takao, M., de Wit, J., Verkerk, A., Eker, A. P., van Leenen, D., et al. (1999). Mammalian *Cry1* and *Cry2* are essential for maintenance of circadian rhythms. *Nature* **398**:627–630.
- Yoo, S. H., Yamazaki, S., Lowrey, P. L., Shimomura, K., Ko, C. H., Buhr, E. D., Siepk, S. M., Hong, H. K., Oh, W. J., Yoo, O. J., Menaker, M., and Takahashi, J. S. (2004). PERIOD2: LUCIFERASE real-time reporting of circadian dynamics reveals persistent circadian oscillations in mouse peripheral tissues. *Proc. Natl. Acad. Sci. USA* **101**:5339–5346.
- Young, M. W., and Kay, S. A. (2001). Time zones: A comparative genetics of circadian clocks. *Nat. Rev. Genet.* **2**:702–715.
- Zeng, H., Hardin, P. E., and Rosbash, M. (1994). Constitutive overexpression of the *Drosophila period* protein inhibits *period* mRNA cycling. *EMBO J.* **13**:3590–3598.
- Zeng, H., Qian, Z., Myers, M. P., and Rosbash, M. (1996). A light-entrainment mechanism for the *Drosophila* circadian clock. *Nature* **380**:129–135.
- Zerr, D. M., Hall, J. C., Rosbash, M., and Siwicki, K. K. (1990). Circadian fluctuations of period protein immunoreactivity in the CNS and the visual system of *Drosophila*. *J. Neurosci.* **10**:2749–2762.
- Zheng, B., Albrecht, U., Kaasik, K., Sage, M., Lu, W., Vaishnav, S., Li, Q., Sun, Z. S., Eichele, G., Bradley, A., and Lee, C. C. (2001). Nonredundant roles of the *mPer1* and *mPer2* genes in the mammalian circadian clock. *Cell* **105**:683–694.

